

## GAIA-CLIM Report / Deliverable D3.6

### Gap Analysis for Integrated Atmospheric ECV CLimate Monitoring:

**Library of (1) smoothing/sampling error estimates for key  
atmospheric composition measurement systems, and  
(2) smoothing sampling error estimates for key data  
comparisons**



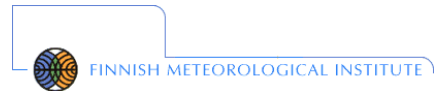
**A Horizon 2020 project; Grant agreement: 640276**

**Date: 15 September 2017**

**Lead Beneficiary: BIRA-IASB**

**Nature: Other**

**Dissemination level: PU**





<b>Work Package</b>	WP 3 – Comparison error budget closure – Quantifying metrology related uncertainties of data comparisons
<b>Deliverable</b>	D3.6
<b>Title</b>	Library of (1) smoothing/sampling error estimates for key atmospheric composition measurement systems, and (2) smoothing/sampling error estimates for key data comparisons
<b>Nature</b>	Other
<b>Dissemination</b>	PU
<b>Lead Beneficiary</b>	Royal Belgian Institute for Space Aeronomy (BIRA-IASB), Brussels, Belgium
<b>Date</b>	15 September 2017
<b>Status</b>	Final, Version 1.0
<b>Editors</b>	Tijl Verhoelst (BIRA-IASB) and Jean-Christopher Lambert (BIRA-IASB)
<b>Contributors</b>	Tijl Verhoelst (BIRA-IASB), Jean-Christopher Lambert (BIRA-IASB) , Alessandro Fassò (UniBG), Fabio Madonna (CNR), Tom Gardiner (NPL), Paul Green (NPL), Gerrit de Leeuw (FMI), Timo Virtanen (FMI), Rigel Kivi (FMI)
<b>Reviewers</b>	Peter Thorne (NUIM)
<b>Contacts</b>	tijl.verhoelst @ aeronomie.be, j-c.lambert @ aeronomie.be
<b>URL</b>	<a href="http://www.gaia-clim.eu/">http://www.gaia-clim.eu/</a>

*This document has been produced in the context of the GAIA-CLIM project. The research leading to these results has received funding from the European Union's Horizon 2020 Programme under grant agreement n° 640276. All information in this document is provided "as is" and no guarantee or warranty is given that the information is fit for any particular purpose. The user thereof uses the information at its sole risk and liability. For the avoidance of all doubts, the European Commission has no liability in respect of this document, which is merely representing the authors' view.*



## Table of Contents

<i>Scope and executive summary</i> .....	4
1. Libraries of ZSL-DOAS and direct-sun total O <sub>3</sub> smoothing and co-location uncertainties (BIRA-IASB).....	6
1.1. Objectives.....	6
1.2. Methodology.....	6
1.3. Library description and user guide .....	8
1.4. Data access.....	11
2. Library of radiosonde <i>T</i> and <i>q</i> temporal mismatch uncertainties (NPL) .....	12
2.1. Objectives.....	12
2.2. Methodology.....	12
2.3. Library description and user guide .....	13
2.4. Data access.....	15
3. Library of IASI-RAOB ( <i>T</i> and <i>q</i> ) space-time co-location uncertainties (UniBG/CNR).....	16
3.1. Objectives.....	16
3.2. Methodology.....	16
3.3. Library description and user guide .....	22
3.4. Data access.....	26
4. Library of AOD spatial and temporal mismatch uncertainties (FMI) .....	27
4.1. Objectives and methodology .....	27
4.2. Library description and user guide .....	28
4.1. Data access.....	29
5. Data set of dedicated GRUAN-processed RS92 launches for co-location with IASI (FMI) ...	30
5.1. Objectives.....	30
5.2. Methodology.....	30
5.3. Data set description and user guide .....	31
6. Conclusion and prospects.....	33
<i>References and related documentation</i> .....	34
<i>Acronyms</i> .....	34
<i>Annex A: Example total O<sub>3</sub> column information sheet</i> .....	36
<i>Annex B: File description for "D3.6_IASI-RAOB_Uncertainty_v2.h5"</i> .....	43
<i>Annex C: File description for "aerosol_uncertainty_library_AERONET_AATSR_*.nc"</i> .....	45
<i>Annex D: Licensing for use of the AERONET data</i> .....	50
<i>Annex E: Full list of GRUAN-processed RS92 launches for co-location with IASI</i> .....	51



## Scope and executive summary

GAIA-CLIM is supporting the European Commission's Copernicus Programme by assessing and improving the fitness-for-purpose of sub-orbital (ground- and balloon-based) reference measurements for the validation of observational data sets from satellites. Amongst others, the project aims at improved traceability and uncertainty characterization of the individual sub-orbital measurement systems, and of the comparison with satellite data. The latter implies the need for a rigorous treatment of so-called co-location mismatch uncertainties. These are the result of (differences in) smoothing and sampling properties of the various ground-based and satellite observing systems. These differences matter because the atmosphere is inhomogeneous and variable on the scale of individual measurements and on the scale of a typical co-location. Consequently, sampling and smoothing differences yield real physical and chemical differences which have nothing to do with the measurement performance per se. Two perfect measurements measuring a slightly different volume and time integral are *a priori* expected to differ.

Within GAIA-CLIM, several methods have been developed for -and applied to- the quantification of smoothing and sampling issues in a range of atmospheric ground-based measurement techniques, and to estimate the uncertainties that need to be taken into account when comparing non-perfectly co-located ground-based and satellite measurements with different spatio-temporal smoothing and sampling properties. The motivation for these developments and the principles of the different methods have been described in deliverable D3.2 ("Generic metrology aspects of an atmospheric composition measurement and of data comparisons"), and a wide variety of applications were performed and reported on in D3.4 ("Measurement mismatch studies and their impact on data comparisons").

To translate these developments and results into a practical, usable resource for C3S users, two avenues were foreseen within GAIA-CLIM: (1) an integration of (derived) tools into the Virtual Observatory, where they serve to estimate smoothing, sampling, and co-location uncertainties for the data ingested into the VO and for the satellite-ground co-locations performed by that system, and (2) publication of libraries (i.e. guiding material and data files) of such uncertainties for key ground-based measurement systems and for key comparisons. The former avenue constitutes the material for deliverables D3.5 and D3.7, while the latter is the topic of the current deliverable, D3.6.

This document complements the actual data files, available for download (by anonymous ftp) at

[ftp://ftp-ae.oma.be/dist/GAIA-CLIM/D3\\_6/](ftp://ftp-ae.oma.be/dist/GAIA-CLIM/D3_6/)

and its purpose is to:

- Define for each library the objective and scope
- Describe briefly the methodology, with references to the related work in D3.2 and D3.4
- Describe the technical aspects of the library, such as file format and contents, best-use practices etc.

More specifically, uncertainty libraries are provided for the following ground-based measurement systems and/or data comparison exercises:



- Ground-based total O<sub>3</sub> column measuring instruments (ZSL-DOAS and direct-sun techniques): horizontal smoothing and co-location uncertainties (Section 1)
- Radiosonde measurements of temperature ( $T$ ) and humidity ( $q$ ): impact of temporal mismatch (Section 2)
- IASI/MetOp vs. radiosonde temperature ( $T$ ) and humidity ( $q$ ) comparisons for a selection of central European radiosonde launching stations (Section 3)
- AOD comparisons between passive ground-based and satellite measurements such as data from the AERONET DRAGON campaign vs. AATSR (Section 4)

Section 5 deals with a somewhat different contribution: it does not present co-location uncertainties but rather a data set of dedicated radiosonde launches (measuring temperature, humidity and occasionally ozone), timed to coincide with IASI/MetOp overpasses, in order to avoid the temporal co-location errors altogether. The launches took place well before the GAIA-CLIM project, but they have now been GRUAN-processed to make them truly reference quality.

The data files presented here, together with the current document, are meant to be a stand-alone result from GAIA-CLIM, with potential use outside the project consortium and beyond the lifetime of the project, e.g. in the context of future C3S-contributing projects. To that end, the data files are already hosted at a location which will remain supported beyond the end of the project. As the libraries presented here are primarily the result of exploratory research, further effort, and corresponding funding, is required to make them more comprehensive: in targeted stations, networks, satellite sounders, ECVs etc., and to make them fit for operational use. This need is included in both the GAID and the recommendations document with further details on potential actors, required budget and time frame.



# 1. Libraries of ZSL-DOAS and direct-sun total O<sub>3</sub> smoothing and co-location uncertainties (BIRA-IASB)

## 1.1. Objectives

The aim of this library is to provide smoothing and co-location uncertainties for every ground-based station hosting (or having hosted) instruments capable of measuring the total column of ozone either in a direct-sun geometry (Brewers, Dobsons, Pandora instruments, and FTIRs) or in a zenith-sky scattered-light geometry (the so-called ZSL-DOAS instruments, for instance the NDACC SAOZ network). A total of 242 ground-based locations are covered.

By smoothing uncertainties, we mean those uncertainties that arise due to the measurement not having an infinitesimally narrow field-of-view at the zenith of the station. Indeed, as described in both D3.2 and D3.4, the actual sensitivity is dispersed along either the line-of-sight towards the sun, or along the light paths before and after the scattering agent at zenith.

By co-location uncertainties, we mean the combined uncertainty resulting from smoothing effects and the imperfect spatio-temporal co-location (in terms of nominal locations) of the ground-based measurement with an independent (e.g. satellite) measurement.

To offer the user a complete and practical set of diagnostics, the following material is provided both in a human-readable information sheet and as netCDF data files, for each station:

- A climatology (1-month resolution) of horizontal smoothing uncertainties/errors, including both random and systematic components, for the ground-based instruments.
- A quantification of the natural spatio-temporal variability of the ozone columns around the station, within the range of typical co-location criteria, for every season.
- Maps of spatial co-location uncertainties/errors (both random and systematic), for every season, assuming a generic co-located (satellite) measurement with a spatial resolution better than 100km.

These libraries can be used both to define, for each station and month or season, appropriate co-location criteria, depending on the maximum allowable co-location mismatch uncertainty, or to interpret/construct *a posteriori* the uncertainty budget of a comparison.

## 1.2. Methodology

The libraries were constructed with the OSSMOSE (Observing System of Systems Simulator for Multi-MissiOn Synergies Exploration) system, developed at BIRA-IASB and described amongst others in GAIA-CLIM deliverables D3.2 and D3.4. The approach consists of a 4-step process:

1. From either detailed radiative transfer calculations or from basic physical principles, observation operators are constructed for the different measurement types. These



observation operators are parametric representations of the full multi-dimensional spatio-temporal sensitivity of a measurement.

2. Using the metadata of actual or hypothetical observations, the observation operators are further specified (i.e. the parameters are given actual values) so as to create 2- or 3-D (or even 4-D) polygons.
3. These observation operators are applied as averaging operators on a gridded representation of the atmosphere, such as a reanalysis, to simulate the smoothed individual measurements.
4. Such simulations are done for a range of ground and/or satellite-based measurements and from these, different analyses can be performed: the co-location mismatch in a comparison can be quantified, a climatology of smoothing errors can be derived, etc.

Specifics for the simulation of total ozone column measurements (and their differences in a satellite validation context) are given in [Verhoelst et al., 2015] For the libraries presented here, OSSSMOSE was used with the MACC (now CAMS) reanalysis ozone fields to perform the following tasks:

- I. Compute horizontal smoothing error climatologies for direct-sun and zenith-sky scattered-light measurements of the total ozone column, by simulating a large set of measurements over a period of 6 years (2005 - 2010), using either the full observation operators, or taking just the zenith column above the station location. The relative smoothing errors are computed as:

$$\varepsilon_{smoothing} = \frac{(TOC_{smoothed} - TOC_{zenith})}{TOC_{zenith}}$$

These smoothing errors were then binned per month to construct the climatology, where the spread within a month can be considered an uncertainty due to the variable nature of the smoothing errors, while the mean is a systematic (at that time scale) error.

- II. Quantify the variability within the reanalysis fields around the station at different spatial ( $\delta r$ ) and temporal ( $\delta t$ ) separations, for a large set of samples over the same 6-year period. The variability is defined as the standard deviation on the differences, where a difference is defined as:

$$\delta TOC =$$

$$TOC(lat_{station} + \delta lat, long_{station} + \delta long, t_0 + \delta t) - TOC(lat_{station}, long_{station}, t_0),$$

where the latitude and longitude offsets are taken to correspond to a given great-circle separation ( $\delta r$ ), at a randomly chosen azimuth ( $\delta \varphi$ ).

- III. Compute full spatial co-location errors around each station per ground-based measurement technique. These errors are defined as:

$$\varepsilon_{co-location, spatial} = \frac{TOC_{zenith}(lat_{station} + \delta lat, long_{station} + \delta long, t_0) - TOC_{smoothed}(lat_{station}, long_{station}, t_0)}{TOC_{smoothed}(lat_{station}, long_{station}, t_0)}$$

The latitude and longitude dimensions are sampled here separately (i.e. not as a combined ( $\delta r$ ) with random ( $\delta \varphi$ ), to retain as much as possible the information on the impact of the highly non-isotropic nature of the smoothing properties of the ground-based measurements.



A few assumptions are implicit in this approach:

- This does not include temporal co-location mismatch, which was found from II) to be of less importance for typical co-location criteria (see next section for illustrations).
- The use of  $TOC_{zenith}$  as the satellite/other measurement implies that this needs to be a measurement with a true (i.e. not just pixel footprint) resolution comparable to (or possibly somewhat better than) that of the model. Otherwise, also the smoothing properties of that measurement need to be considered. To keep the results presented in these libraries as generic as possible, it was decided not to include any smoothing on the satellite measurement. For current-day sensors such as GOME-2 on MetOp-A and MetOp-B, this was found to be a reasonable approximation as long as the SZA of the measurement is below about  $75^\circ$  [Verhoelst et al.,2015]. This also holds for most future sensors which will in general have even better nominal resolution, as long as solar zenith and viewing angles are moderate.

### 1.3. Library description and user guide

The libraries consist of two types of material:

- 1) Information sheets in .pdf format, one per station hosting (or having hosted) a total ozone column measuring instrument and offering their data either through the WOUDC or the NDACC archive (242 stations covered). These information sheets contain figures of the results described under I. through III. in the section above. An example of such an information sheet is provided as Annex A.
- 2) netCDF files, containing the data behind the figures in the information sheets, meant to allow the user to ingrate the results in their own analysis. Three types of files are available:
  - a. `TOC_stationName_measurementType_SmoothingErrors.nc` containing the horizontal smoothing error climatology:  $\sigma(\varepsilon_{smoothing})$  and  $\mu(\varepsilon_{smoothing})$ .
  - b. `TOC_stationName_NaturalVariability.nc` containing the climatology of natural spatio-temporal variability around the station within the range of typical co-location criteria:  $\sigma(\delta TOC(dr, dt))$
  - c. `TOC_stationName_measurementType_CoLocationUncertainty.nc` containing the climatology of spatial co-location uncertainty (i.e. smoothing + offset in nominal locations):  $\sigma(\varepsilon_{co-location,spatial})$  and  $\mu(\varepsilon_{co-location,spatial})$ .

The first type of data file allows the user to associate with a ground-based measurement both a random uncertainty (the reported spread on the smoothing errors) and a systematic error (the reported mean of the smoothing errors) due to horizontal smoothing effects. This corresponds to the 1<sup>st</sup> type of figure in the information sheet, an example of which is shown in Figure 1.



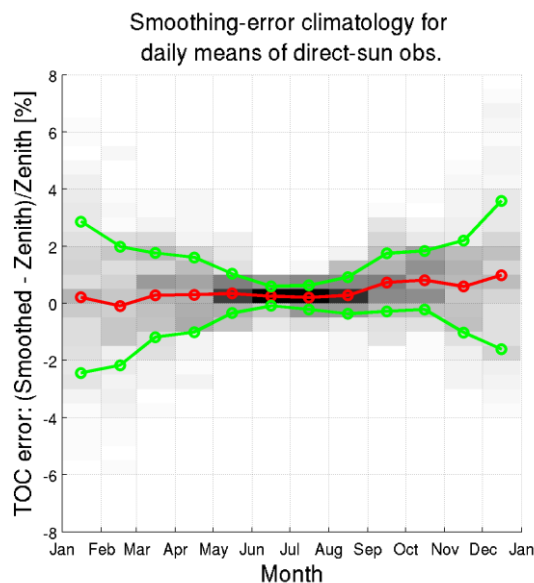


Figure 1: Horizontal smoothing error climatology for daily means of direct-sun observations (from e.g. Dobsons or Brewers) at Arosa (CH). The red curve (mean error) and green curves (standard deviation of the errors) are provided in the netCDF data files `TOC_stationName_measurementType_SmoothingErrors.nc`.

The 2<sup>nd</sup> type of data file allows the user to get a quantified estimate of the natural variability at a certain distance and time difference around a ground-based measurement. This can inform for instance the co-location criteria in a validation exercise, where a satellite is required to coincide with the ground-based measurement within a  $(dr, dt)$  combination that ensures an acceptably low contribution by natural variability, but without taking into account the specific smoothing properties of the ground-based measurement. This corresponds to the 2<sup>nd</sup> type of figure in the information sheet, an example of which is shown in Figure 2.

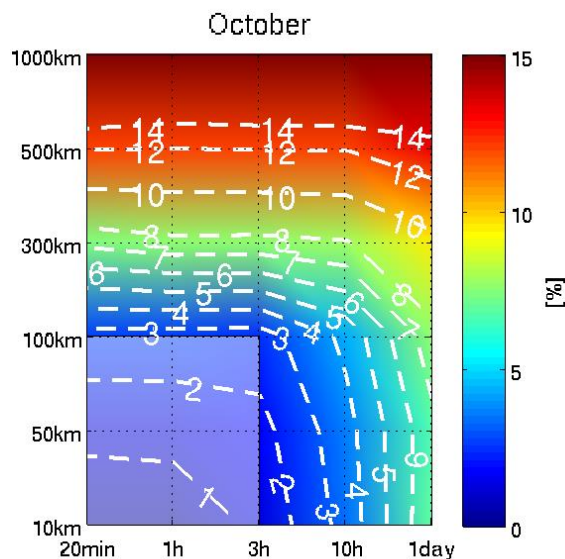


Figure 2: Climatology of natural variability in the TOC field around the Rothera station (Antarctica) in local spring, as a function of temporal (x-axis) and spatial (y-axis) separation. These data are available in the netCDF data files named `TOC_stationName_NaturalVariability.nc`

The 3<sup>rd</sup> type of data file allows the user to further minimize (or better characterize) spatial (i.e. excluding the temporal component) co-location mismatch uncertainties by including the smoothing properties of the ground-based measurement, and by differentiation of spatial separation into the latitude and longitude dimensions. The latter allows the user to take into account the non-isotropic nature of the ozone field. This data file corresponds with the 3<sup>rd</sup> type of figure in the information sheets, an example of which is shown in Figure 3.

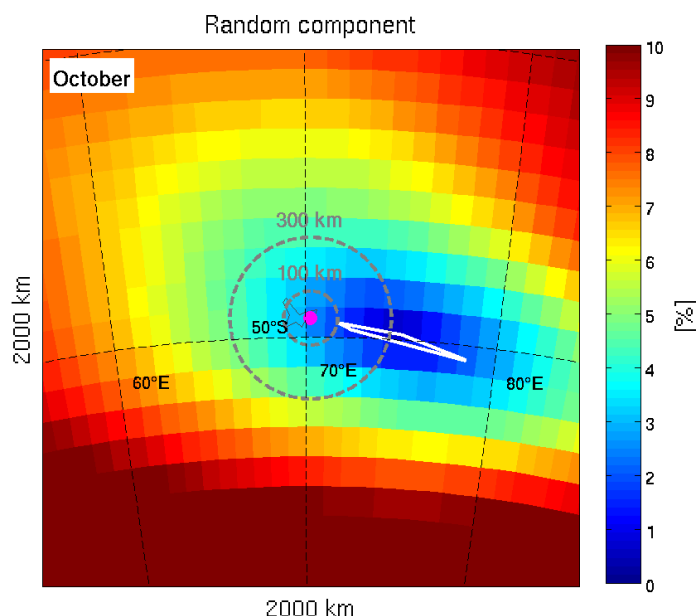


Figure 3: Climatology of the random component of the spatial co-location uncertainty for sunrise ZSL-DOAS measurements at Kerguelen (Southern Indian Ocean) in local spring. These type of data are available in the netCDF data files named `TOC_stationName_measurementType_CoLocationUncertainty.nc`.

This 3<sup>rd</sup> type of library already combines the spatial information of the 1<sup>st</sup> and 2<sup>nd</sup> type of files, meaning that only the temporal co-location uncertainty still needs to be added to construct the total co-location uncertainty. For now, this can be done by adding –in quadrature– to the uncertainty from the 3<sup>rd</sup> library the value at  $dr=0$  from the 2<sup>nd</sup> library. The total co-location uncertainty, to which only the measurement uncertainties still need to be added (also in quadrature), then becomes:

$$\sigma(\varepsilon_{co-location}) = \sqrt{\sigma^2(\varepsilon_{co-location,spatial}) + \sigma^2(\delta TOC(0, dt))}$$

In a future release of the library, a 4<sup>th</sup> type of file will be provided, including the temporal component for different time differences.

The structure of the netCDF files is designed to be self-explanatory.

### Known issues and foreseen upgrades (on 15 September 2017):



- Combined spatio-temporal co-location uncertainty, including smoothing effects, is still to be constructed for a range of time differences, i.e. the 4<sup>th</sup> type of library discussed in the previous section.
- Impact of orography (high-altitude stations) still needs to be implemented
- For Brewers: Differentiation between single and double monochromators (and resulting limiting SZA range) still to be implemented. Direct-sun measurements are now assumed to be possible only at SZA<80°.

This work will be performed on a best-effort basis in the remaining time of GAIA-CLIM, and it will be reported on in an update of this deliverable made available with the data files on the server referenced in the next section.

## 1.4. Data access

The high-level access point for this data set, both information sheets and netCDF data files, is:

[ftp://ftp-ae.oma.be/dist/GAIA-CLIM/D3\\_6/Ozone/BIRA/](ftp://ftp-ae.oma.be/dist/GAIA-CLIM/D3_6/Ozone/BIRA/)

Subdirectories for information sheets and netCDF data files are self-explanatory.



## 2. Library of radiosonde $T$ and $q$ temporal mismatch uncertainties (NPL)

### 2.1. Objectives

The accompanying spreadsheets provide data to enable estimation of the co-location uncertainty in non-simultaneous temperature and humidity measurements due to atmospheric variability, both in terms of the systematic bias between measurements and the random noise. The availability of such data provides an estimate of temperature and humidity mismatch uncertainties for the given sites using global reanalysis data and sonde measurement data (where available). This enables an appropriate sampling strategy to be put in place for a given intercomparison measurement application in order to meet a defined comparison uncertainty requirement.

Previous work (Determining the temporal variability in atmospheric temperature profiles measured using radiosondes and assessment of correction factors for different launch schedules [Butterfield & Gardiner, 2015]) established that 4 launches per day (or 6 hourly updates) provided a reasonable measure of the variability during the day. It also provided estimates from actual sonde datasets, as a function of time of day, altitude and season – but only for temperature and for the very limited number of GCOS Reference Upper Air Network (GRUAN) sites that provide long-term data at the required high level of sonde launch frequency. The work within GAIA-CLIM has extended this analysis to cover humidity; included additional uncertainty assessments using the reported measurement uncertainties in the GRUAN sonde data; and extended the coverage of the analysis, through the use of ECMWF ERA Interim re-analysis data, to provide a globally-applicable co-location uncertainty assessment tool.

### 2.2. Methodology

The mismatch uncertainties are reported as a function of pressure for 32 levels from 1000 hPa up to 10 hPa, corresponding to the reported pressure levels in the ERA Interim re-analysis data. The radiosonde temperature readings are averaged over the readings within  $\pm 0.5$  hPa of the pressure level value to provide a mean temperature,  $T$ , for that specific level. The rate of change in temperature between single launches 6 hours apart, at each level, were calculated according to Eqn (2.1). The mean rate of change in temperature between each launch separation,  $\frac{dT}{dt_n}$ , for a defined group of launches were then calculated according to Eqn (2.2).

$$\frac{dT}{dt_n} = \frac{T_n - T_{n-1}}{t_n - t_{n-1}} \quad (2.1)$$

Where  $t_n$  is the launch time for the sonde.

$$\overline{\frac{dT}{dt_n}} = \frac{\sum \frac{dT}{dt_n}}{i} \quad (2.2)$$



Where  $i$  = the number of launch pairs.

The result of this calculation provides the mean rate of change of temperature as a function of altitude for launches grouped by time of day and season across the datasets being investigated, with the standard error on the mean providing a measure of the random uncertainty resulting from the variability observed for that particular grouping.

An identical calculation of mean rates of change, and the associated standard error on the mean, was performed for the relative humidity data from the GRUAN radiosonde and ERA-Interim results.

## 2.3. Library description and user guide

The temporal mismatch data is provided in 5 MicroSoft Excel workbooks:

- Temperature\_ECMWF\_v1.xlsx
- Temperature\_GRUAN\_v1.xlsx
- Humidity(Ice)\_ECMWF\_v1.xlsx
- Humidity(Water)\_ECMWF\_v1.xlsx
- Humidity(Water)\_GRUAN\_v1.xlsx

where the file title gives the mismatch parameter, the data source, and the data version. Note that two ECMWF humidity results are provided for relative humidity either calculated over water or over ice. The ECMWF ERA Interim output provides relative humidity over ice, whilst sonde data provide relative humidity over water. The ECMWF relative humidity over water has been calculated from ECMWF specific humidity and temperature data and the Vaisala documentation (which follows Hyland & Wexler).

Within each workbook are a series of worksheets, each providing the results for a particular site. In the case of the GRUAN sonde data there are two sites – Lindenberg and Southern Great Plains – while the ECMWF analysis had been extended to cover 10 GRUAN sites. The name, location and elevation of these sites is given in Table 2.1 below.

**Table 2.1 Location of GRUAN sites selected for ERA-Interim Analysis**

Location	Latitude	Longitude	Elevation [m.a.s.l.]
Barrow	71.32° N	156.61° W	8
Boulder	39.95° N	105.20° W	1743
Lauder	45.05° S	169.68° E	370
Lindenberg	52.21° N	14.12° E	98
Manus	2.06° S	147.42° E	6
Ny Alesund	78.92° N	11.92° E	5
Potenza	40.60° N	15.72° E	720



Southern Great Plains	36.60° N	97.49° W	320
Sodankyla	67.37° N	26.63° E	179
Tateno	36.06° N	140.13° E	31

Each worksheet identifies the site, the parameter being assessed, the period over which the data has been analysed, the data source (ECMWF or GRUAN), and the local time at the site relative to UT (ignoring daylight saving adjustments).

The main data section then gives the mean rates of change of the assessed parameter, the estimated noise on these rates of change and the number of data points used to calculate the rates of change. These are provided at a series of 32 fixed pressure levels across the atmospheric column from 10 hPa to 1000 hPa – note that, if data are not available at a particular level, ‘NaN’ is entered in the data cells for that level.

Rate of change profiles are given ‘By Launch Time’ to show how the rates change at different times of day, and are further broken down ‘By Season, By Launch Time’ to show the seasonal variation in the rate of change behaviour. Note that the Season definitions are based on Northern Hemisphere seasons, so Spring covers Mar/Apr/May, Summer covers Jun/Jul/Aug, Autumn covers Sep/Oct/Nov and Winter covers Dec/Jan/Feb.

In terms of use of the mismatch data, the mean rate of change results provide the underlying systematic temporal co-location difference in K/hr or %RH/hr for the given location, time of day, and season. This systematic rate of change will not be reduced by repeated measurements, and because these results provide an estimate of its value it can be corrected for in a co-location experiment.

The estimated noise on the rate of change gives information on the random component of the co-location uncertainty that will be reduced by repeated measurements. Each estimated noise value given in the worksheets is the standard deviation (in K or %RH) of the mean result for the number of data points for that particular result ( $N_r$ ). Therefore, to estimate the random component of temporal co-location uncertainty for a new dataset with  $N_x$  points, the noise value in the worksheet ( $\sigma_r$ ) should be multiplied by a factor of  $\left(\frac{\sqrt{N_r}}{\sqrt{N_x}}\right)$ . Alternatively, the same relationship can be used to predict the number of co-location data points ( $N_t$ ) required to meet a target uncertainty level ( $\sigma_t$ ), given by:

$$N_t = N_r \left(\frac{\sigma_r}{\sigma_t}\right)^2$$

Besides these data files, also visualizations are provided as figure (.png) files. These plots provide a graphical representation of the temperature and humidity mismatch profiles for the different sites, with a separate plot for each season. The solid lines show the mean difference in temperature or relative humidity between ECMWF ERA Interim results 6 hours apart at different times of day (N.B. all times are in local time ignoring daylight saving adjustments), and the error bars show the standard deviation of the mean result. An example is shown in Figure 4.

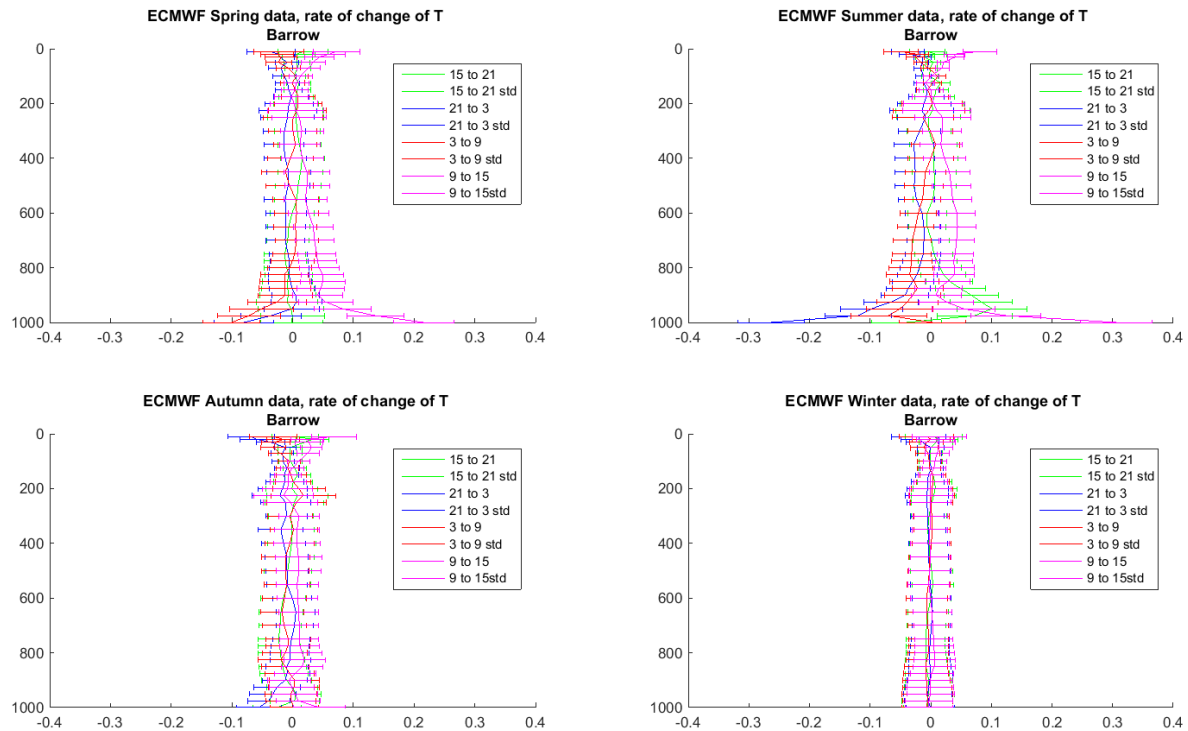


Figure 4: Rate of change in temperature (K/hr) at Barrow, Alaska, as derived from multiple daily radiosonde launches. Different colours refer to different times of day.

## 2.4. Data access

The high-level access point for this data set, both spreadsheets and figures, is:

[ftp://ftp-ae.oma.be/dist/GAIA-CLIM/D3\\_6/TempHum/NPL/](ftp://ftp-ae.oma.be/dist/GAIA-CLIM/D3_6/TempHum/NPL/)

Subdirectories for spreadsheets and figures are self-explanatory.

Although this data has initially been provided in Excel spreadsheets a version in NetCDF format will also be produced.



## 3. Library of IASI-RAOB ( $T$ and $q$ ) space-time co-location uncertainties (UniBG/CNR)

### 3.1. Objectives

The objective of this library is to allow quantification of the co-location uncertainties for comparisons between GRUAN soundings (or more generally any  $T$  and  $q$  measuring radiosonde) and IASI satellite measurements of the temperature and humidity profile. Besides the imperfect spatio-temporal co-location, also the difference in vertical resolution (smoothing) has to be dealt with. In D3.4, we described in detail the statistical methods used to quantify first the optimal vertical smoothing, including the resulting uncertainties, and thereafter the spatio-temporal co-location mismatch uncertainties. Some further refinements, developed between delivery of D3.4 and the current deliverable, are described below:

- 1) B-splines have been used for RAOB profiles instead of Hermite splines, which were used in D3.4. This gives a better fitting in terms of GRUAN-RAOB error.
- 2) A new penalized optimization algorithm has been introduced in the weighting functions. In fact, the weighting functions, used in Section 3.1.2 to understand IASI vertical smoothing, are assumed to change smoothly when moving from one pressure level to the next one. Instead in D3.4 the weighting functions were assumed independent at different levels. The new approach reflects the physical aspect related to atmospheric smoothness and is thus preferable.
- 3) Spatio-temporal mismatch uncertainty is based on distance in space instead of air distance, which was used in D3.4. Since the results of both are quite close, in the present LUT's, for user convenience, the simplest approach is implemented.

Although above ameliorations gave better results, they are, generally speaking, similar to those outlined within D3.4.

### 3.2. Methodology

This section explains how the uncertainties are estimated. As explained in D3.4, in order to have an appropriate spatio-temporal resolution, the analysis is not limited to GRUAN-IASI comparison but involves RAOB-IASI comparison. The estimation procedure, based on temperature and humidity data in a region of continental Europe, is organized in the following steps:

- i) Since RAOB products have a limited vertical resolution, they are transformed in B-splines data and their information content is assessed by comparing RAOB and GRUAN products where available. As a result of this assessment, two additional uncertainties are defined: a sparseness uncertainty and a processing uncertainty.
- ii) IASI vertical smoothing is assessed by an independent method which does not rely on averaging kernels. To do this, sonde measurements are harmonized in order to match approximately the vertical smoothing of IASI products. The vertical smoothing uncertainty is then defined as the



difference between the total co-location uncertainty and the co-location uncertainty using the harmonized RAOB data.

- iii) Using the harmonized data, the joint impact on co-location uncertainty profile of distance and time difference between the two products is considered giving nighttime and daytime results.

The RAOB-IASI dataset considered here covers the central European area (C-EU) (Figure 5) for the period January 2015 – February 2016. The co-locations have been provided by NOAA through the NPROVS system, and are discussed in more detail in D3.4. In addition, also the continental GRUAN stations at Cabauw, Lindenberg, Payerne and Sodankyla have been considered. The NOAA NPROVS system provided also IASI retrieval uncertainties, but individual averaging kernels were not made available in this dataset. For this reason, the averaging kernels have not been used here.

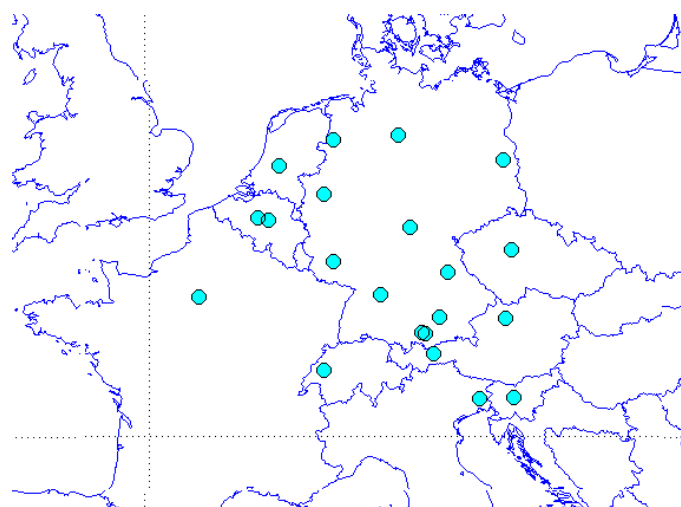


Figure 5: Central European RAOB network (C-EU) including three continental GRUAN stations at Cabauw, Lindenberg and Payerne.

### **Vertical smoothing**

RAOB and IASI profiles are not immediately comparable because they are not available at the same pressure levels and, more importantly, have different vertical smoothing properties. In fact IASI observations, due to kernel averaging, have an important vertical smoothing, which is essentially absent in radiosonde products.

For these reasons, the approach reported below has the aim to reconcile the difference in smoothing properties between the two products and, then, to assess the co-location uncertainty after considering sparseness and vertical smoothing uncertainties.

For a given co-location  $k$ , let  $\mathbf{x}_G$  be the RAOB  $N_k$ -dimensional vector of the measurements made at the  $N_k$  pressure levels  $\mathbf{p}_G = (p_{G,1}, \dots, p_{G,N_k})$ , moreover, let  $\mathbf{x}_S$  be the IASI measurement vector related to the  $M$  pressure levels  $\mathbf{p}_S = (p_{S,1}, \dots, p_{S,M})$ .

Since RAOB and IASI measurements are not available at the same pressure levels, that is  $p_{G,l} \neq p_{S,h}, l = 1, \dots, N_k, h = 1, \dots, M$ , in the next section, RAOB raw profiles are transformed into



continuous profiles in order to have estimates at the IASI levels  $p_S$  and to define a transform of RAOB with smoothing properties similar to IASI.

### Sparseness and processing uncertainty

Discrete RAOB profiles  $x_G$  have been transformed into continuous profiles  $x_G^S$  using penalized B-splines. In order to assess the accuracy of the RAOB splines in terms of vertical information reconstruction, the interpolated RAOB are validated using the GRUAN dataset, which covers the same period and a subset of RAOB stations, namely Cabauw, Lindenberg and Payerne. For this reason, validation is based only on 306 launches for temperature and 439 launches for WVMR.

The spline uncertainty is assessed by considering the difference between RAOB splines and high resolution GRUAN measures,  $x_G^S - x_{ref}$ . Hence the B-spline smoothing coefficient is computed by minimizing the GRUAN-RAOB mean square difference. Figure 6 and Figure 7 show the uncertainty

$$\sqrt{E(x_G^S - x_{ref})^2}$$

at various pressure levels. Minima of the graph are the mandatory pressure levels, where there is always a RAOB measure. Note that these minima are not zero as GRUAN retrievals are obtained using GRUAN processing, which is different from the Vaisala processing, used in the RAOB dataset, see Dirksen et al. (2014) for details. Once this Vaisala processing uncertainty is eliminated the remaining part is related to lack of information of RAOB products related to vertical sparseness. For temperature, in the range 1000-300 hPa this is smaller than 0.4 K but increases to about 0.8 K in upper reaches of the measured profile. For humidity this is smaller than around 0.3 g/kg up to 500 hPa and smaller than 0.1 g/kg above (although note that relative uncertainty increases as the absolute humidity decreases by two orders of magnitude over a typical profile from the surface up to burst-point). Note that, this improves over Hermite splines used in D3.4.

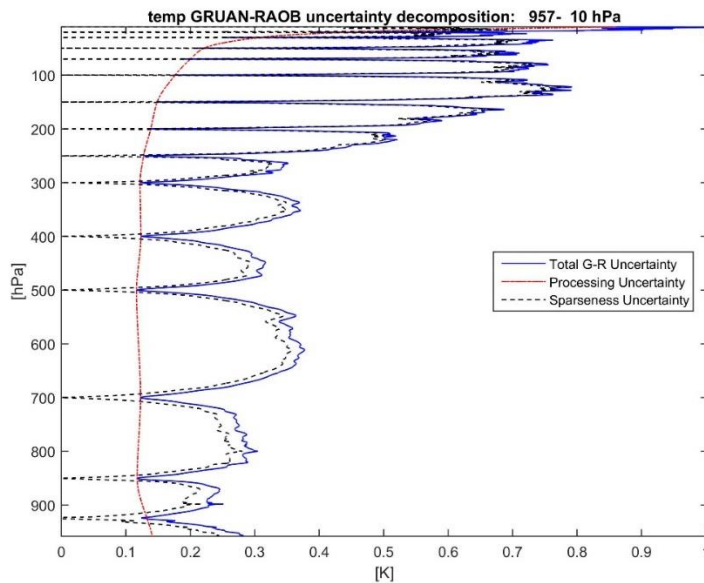


Figure 6: B-Spline interpolation uncertainty for temperature, assessed through GRUAN-RAOB comparison. The blue solid line is given by  $\sqrt{E(x_G^S - x_{ref})^2}$ . The red dot-dashed line is given by local minima of interpolation



uncertainty which occur at mandatory levels: 925, 850, 700, 500, 400 hPa. The black dashed line is the quadratic difference of the previous two uncertainties.

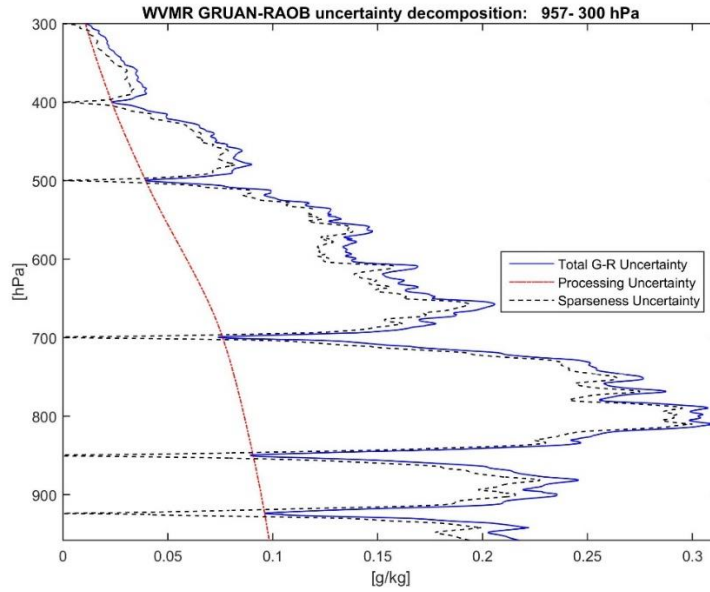


Figure 7: Spline interpolation uncertainty for WVMR, assessed through GRUAN-RAOB comparison. The blue solid line is given by  $\sqrt{E(x_G^S - x_{ref})^2}$ . The red dot-dashed line is given by local minima of interpolation uncertainty which occur at mandatory levels: 925, 850, 700, 500, 400 hPa. The black dashed line is the quadratic difference of the previous two uncertainties.

### Vertical smoothing uncertainty

In the comparison of co-located RAOB-IASI profiles, we consider that the different vertical smoothness of the two data products contributes to the total co-location uncertainty. In order to assess the vertical smoothing uncertainty, we first approximate the IASI vertical smoothing properties, solving an optimization problem.

To see this, we introduce the smoothed RAOB measure at pressure level  $p_{S,h}$ , which is given by

$$\tilde{x}_{G,h}^S(\boldsymbol{\theta}) = \int x_G^S(p)w(p; \boldsymbol{\theta})dp$$

where  $w(p; \boldsymbol{\theta})$  is a normalized weight function with parameter vector  $\boldsymbol{\theta}$ . In D3.4, weight functions with different shapes have been tested and it was found that best results are obtained by the generalized extreme value (GEV) density function which is characterized by three parameters, so that  $\boldsymbol{\theta} = (\text{shape}, \text{scale}, \text{position})$ .

For each pressure level  $p_{S,h}$ , the parameter vector  $\boldsymbol{\theta}$  is obtained by minimizing the distance between IASI  $x_{S,h}$  and smoothed RAOB  $\tilde{x}_{G,h}^S$ . To do this, consider  $K$  different RAOB-IASI co-location profiles observed across space and time and let  $E()$  be the average operator over these  $K$  co-locations. Hence the optimal smoothing is given by the iteration for  $h = 1, \dots, M$  of the following penalized minimum co-location mean square error problem:



$$\hat{\theta}_h = \underset{\theta}{\operatorname{argmin}} \left( E \left[ (x_{S,h} - \tilde{x}_{G,h}^S(\theta))^2 \right] + I(h > 1) \frac{\|\theta - \hat{\theta}_{h-1}\|}{\sigma_\theta} \right)$$

where  $\frac{\|\theta - \hat{\theta}_{h-1}\|}{\sigma_\theta}$  is the penalization term which reflects atmospheric smoothness and prevents  $\theta$  to vary excessively from a pressure level to the next. The quantity

$$\tilde{x}_{G,h}^S = \tilde{x}_{G,h}^S(\hat{\theta}_h)$$

is the RAOB transformed to mimic IASI smoothing properties. Additionally, the vertical smoothing uncertainty at pressure level  $p_{S,h}$  is given by

$$u_{v,smooth}^2 = E \left[ (\tilde{x}_{G,h}^S - x_{G,h}^S)^2 \right]$$

and, in practice, it can be computed by

$$u_{v,smooth}^2 = u_{tot}^2 - u_{adj}^2$$

where  $u_{tot}$  is the total co-location uncertainty at pressure level  $p_{S,h}$ , which includes differences in horizontal and temporal co-location, as well as differences in vertical smoothing, that is:

$$u_{tot}^2 = E \left[ (x_{S,h} - x_{G,h}^S)^2 \right].$$

Moreover,  $u_{adj}$  is the adjusted co-location uncertainty, corrected for differences in vertical smoothing, that is:

$$u_{adj}^2 = E \left[ (x_{S,h} - \tilde{x}_{G,h}^S)^2 \right].$$

### Analysis and results

Figure 8 and Figure 9 show the shape of the GEV functions for a subset of the IASI pressure levels, giving information on IASI smoothing at different altitudes. Note that the above results are valid independently of the date, hour, location and meteorological conditions in the NPROVS dataset used. In fact, we considered also more detailed models where the GEV parameter  $\theta$  is allowed to vary as a function of latitude, longitude, day effect, seasonal effect and geopotential height at 500 hPa, but no significant improvement was found. This means that the above results are quite stable and that there would be little value in additional complexity of providing more complicated tables for this effect that varied seasonally, daily or by location over this domain. This may not hold true for additional domains such as tropical or polar latitudes.

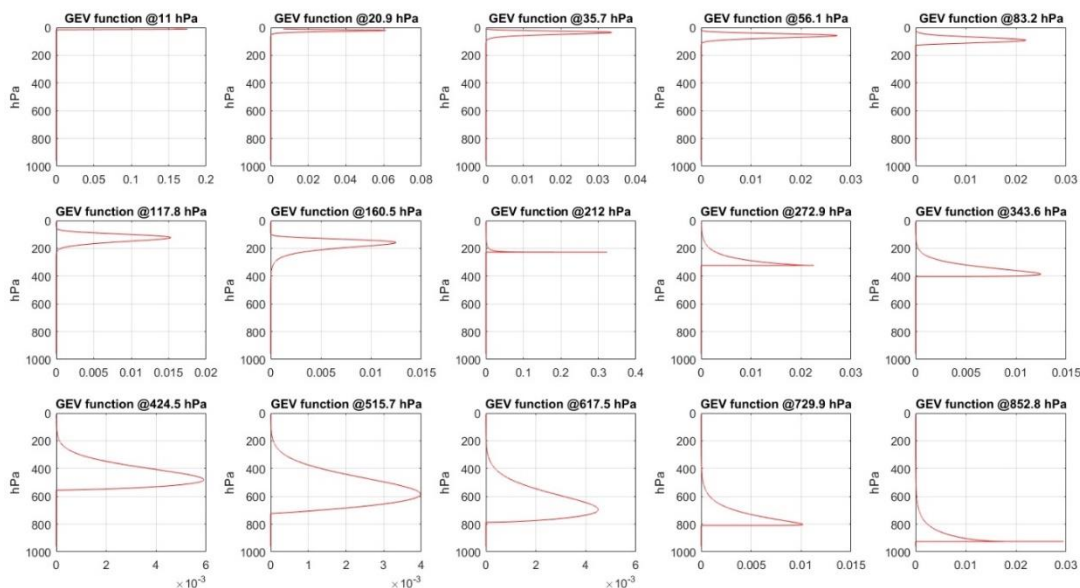


Figure 8: GEV weight functions for temperature at selected of IASI pressure levels.

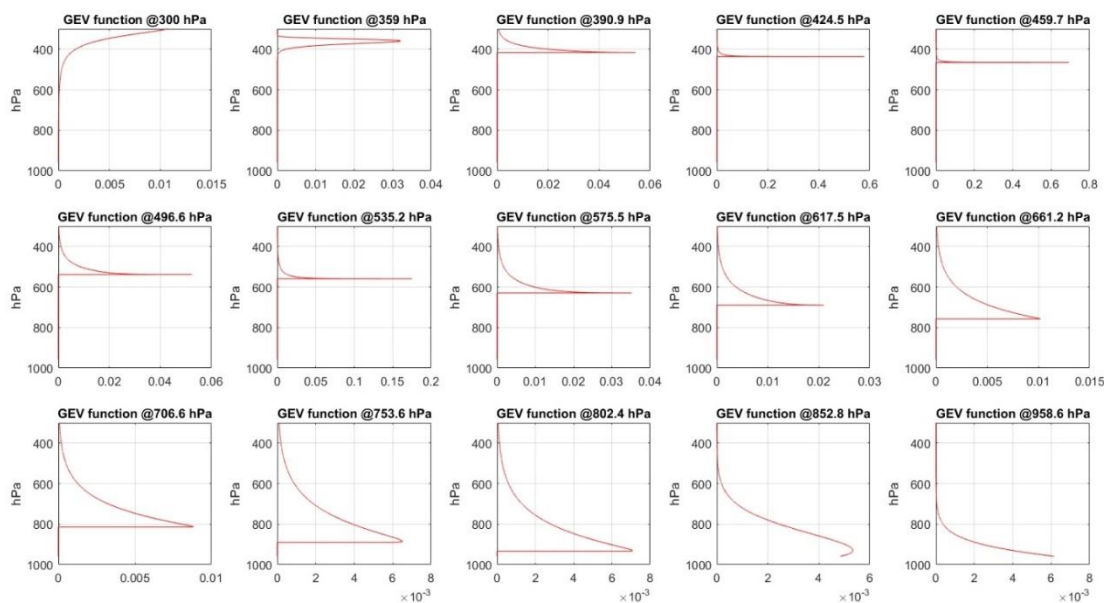


Figure 9: GEV weight functions for WVMR at selected of IASI pressure levels.

The RAOB data, harmonized to IASI smoothing by the above GEV weight functions, are used to evaluate both the vertical smoothing uncertainty  $u_{v,smooth}^2$  and the adjusted co-location uncertainty  $u_{adj}^2$ . The corresponding uncertainty decomposition is displayed in Figure 10 and Figure 11, which show that both total co-location uncertainty,  $u_{tot}$ , and vertical smoothing uncertainty,  $u_{v,smooth}$ , have the same oscillating behavior with local minima at mandatory levels as in Figure 6 and Figure 7 due to the sparseness uncertainty already discussed. Interestingly, this effect is largely reduced in the co-location uncertainty  $u_{adj}$ .



### ***Spatio-temporal mismatch uncertainty***

In this section, we consider the effect of spatial and temporal mismatch to the co-location uncertainty of the previous section. In particular, the vertically harmonized RAOB of the previous section are considered with a focus on the co-location mean square error

$$u_{adj}^2 = E \left[ (x_{s,h} - \tilde{x}_{G,h}^S)^2 \right]$$

where, as before,  $x_{s,h}$  is IASI temperature or humidity and  $\tilde{x}_{G,h}^S$  is the corresponding smoothed RAOB measurement.

The objective here is to understand the variation of the above co-location uncertainty as a function of the horizontal distance between IASI and RAOB measurements at each IASI pressure level  $p_{s,h}$ , that is

$$u_{adj}^2 = \sigma^2(\partial s, \partial t)$$

where  $\partial s$  is the distance in space while  $\partial t$  is the time difference between measurements. D3.4 considered air mass distance instead of distance in space obtaining close results. We use distance in space here for user convenience.

Since, from physical considerations, we may assume that  $\sigma^2(\partial s, \partial t)$  is a nondecreasing function in each of its coordinates, we estimate the function  $\sigma^2(\partial s, \partial t)$  by fitting a bidimensional isotonic regression model to squared co-location errors

$$\epsilon_h^2 = (x_{s,h} - \tilde{x}_{G,h}^S)^2$$

at each pressure level  $p_{s,h}$ .

The bidimensional isotonic regression technique is a constrained least squares method, which gives an estimate of  $\sigma^2$  such that  $E(\sigma^2 - \epsilon^2)^2$  is a minimum, conditional on marginal monotonic constraints, that is  $\sigma^2(\partial s + d, \partial t) \geq \sigma^2(\partial s, \partial t)$  and  $\sigma^2(\partial s, \partial t + d) \geq \sigma^2(\partial s, \partial t)$  for any  $d > 0$ .

The isotonic model, fitted separately to daytime and nighttime co-locations, gives the LUT's of Section 3.3 Figure 12 and Figure 13 illustrate this estimated uncertainty at 931.5 hPa for temperature and humidity respectively.

## **3.3. Library description and user guide**

File D3.6\_IASI-RAOB\_Uncertainty.h5 is an hdf5 file which contains vertical smoothing uncertainty and spatio-temporal mismatch uncertainty for temperature and water vapor mixing ratio (WVMR). The full netcdf structure is reported in the Appendix but summarized here. More specifically, the file contains two variables:

- Temperature
- Wvmr

with different units [K] or [g/Kg], but equal structure:

- Day
- Night
- VerticalSmoothing



The groups Day and Night contain information on spatio-temporal mismatch uncertainty, while the group VerticalSmoothing contains information about vertical smoothing uncertainty. The definition of the exact file format (variable names etc.) is provided in [Annex B](#).

### Vertical smoothing uncertainty

Vertical smoothing uncertainty is the part of total co-location mismatch uncertainty due to IASI vertical smoothing. As derived in Section 3.2, this quantity, denoted by  $u_{v.smooth}$ , is given by

$$u_{v.smooth}^2 = u_{tot}^2 - u_{adj}^2$$

where  $u_{tot}$  is the total co-location mismatch uncertainty and  $u_{adj}$  is the adjusted co-location uncertainty, corrected for differences in vertical smoothing.

The group VerticalSmoothing contains the following datasets:

- VSmoothingUncertainty (75×1) [K] or [g/kg]
- pressureLevel (75×1) [hPa]

where pressureLevel contains the IASI pressure levels.

As an illustration, the vertical smoothing uncertainty and its components are reported in Figure 10 and Figure 11 for temperature and humidity respectively.

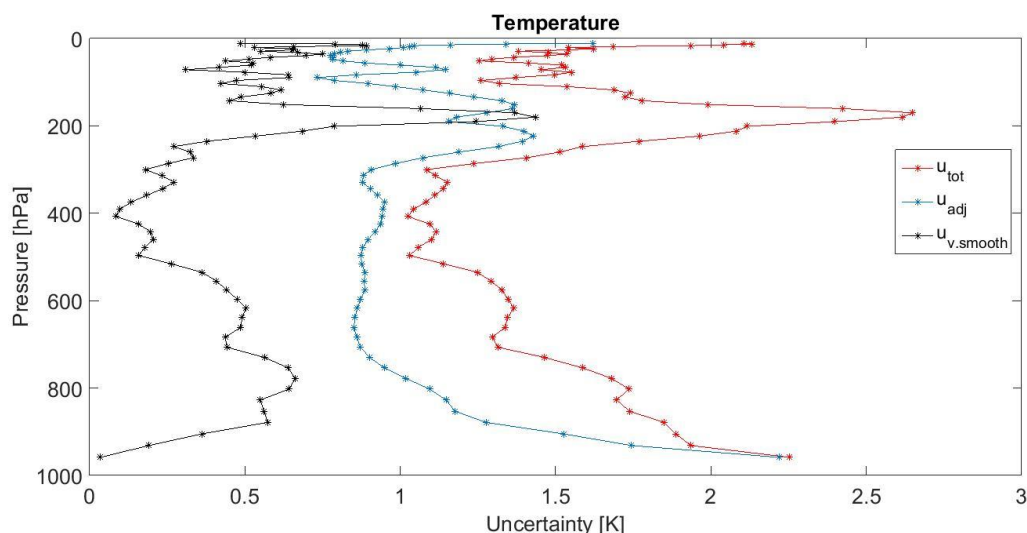


Figure 10: Uncertainty decomposition for temperature. The red curve is the total co-location uncertainty  $u_{tot}$ , the blue curve is the adjusted co-location uncertainty  $u_{adj}$  while the black curve is the vertical smoothing uncertainty  $u_{(v.smooth)}$ , such that  $u_{(v.s$

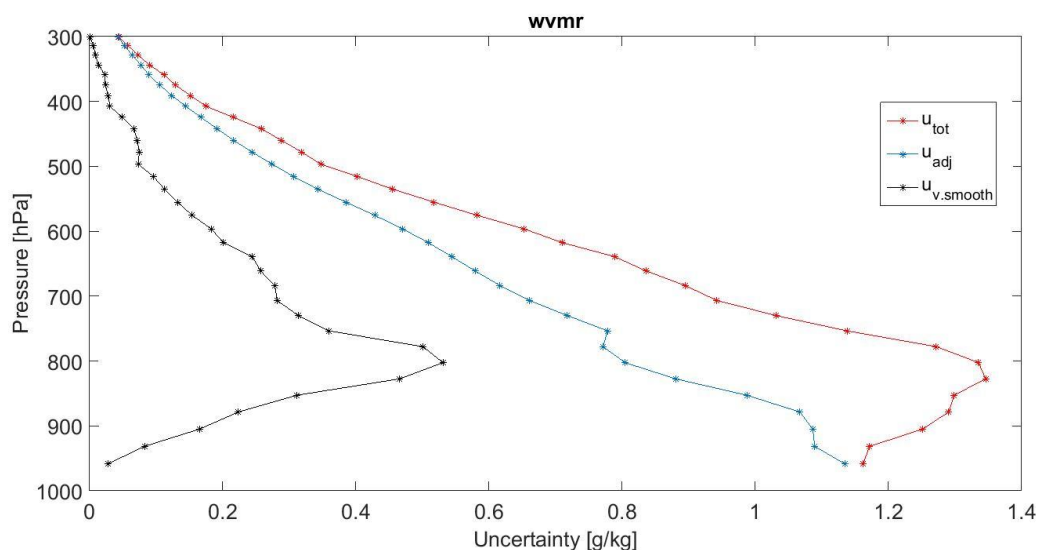


Figure 11: Uncertainty decomposition for WVMR. The red curve is the total co-location uncertainty  $u_{tot}$ , the blue curve is the adjusted co-location uncertainty  $u_{adj}$  while the black curve is the vertical smoothing uncertainty  $u_{v.smooth}$  such that  $u_{v.smooth}^2$

### ***Spatio-temporal mismatch uncertainty***

The groups Day and Night give the contributions to the co-location mismatch uncertainty at a certain distance and a certain time difference between sonde and IASI measurements. In particular the LUT's of this Section report the net co-location uncertainty after adjusting for vertical smoothing. This means that the uncertainty  $u_{adj}$  is seen as a function of distance in space and time difference  $(\partial s, \partial t)$  :

$$u_{adj} = u(\partial s, \partial t).$$

In particular groups Day and Night contain the datasets

- colocDistance (101×1) [Km]
- colocTimeDifference (101×1) [h]
- colocUncertainty (75×101×101) [K] or [g/kg]
- pressureLevel (75×1) [hPa]

Hence, for each combination of pressureLevel, colocDistance and colocTimeDifference, the corresponding value of colocUncertainty gives the spatio-temporal mismatch uncertainty.

As an illustration, the net co-location uncertainty at 931.5 hPa is reported in Figure 12 and Figure 13 for temperature and humidity respectively.



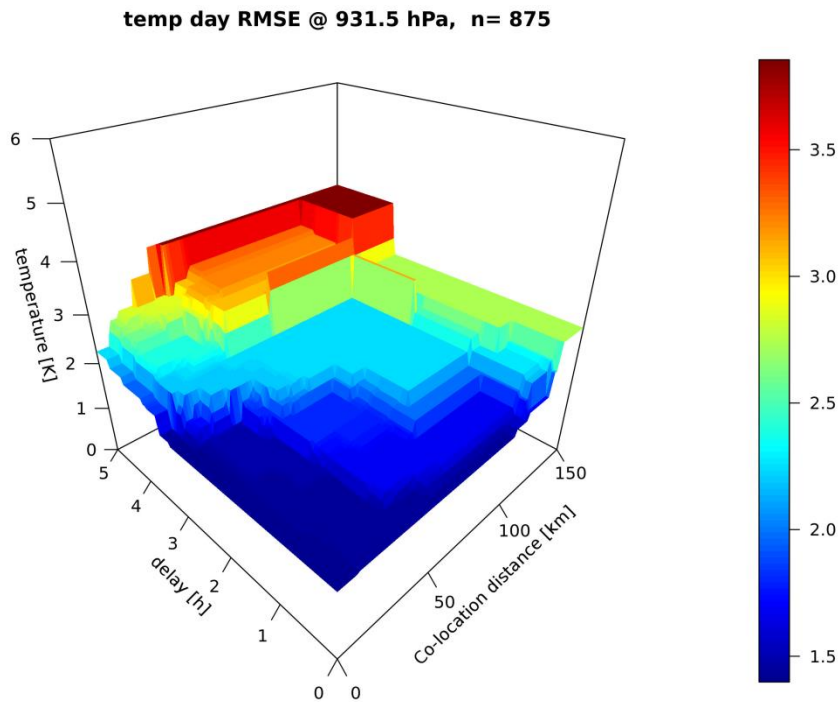


Figure 12: Net co-location uncertainty for temperature, daytime, at 931.5 hPa.

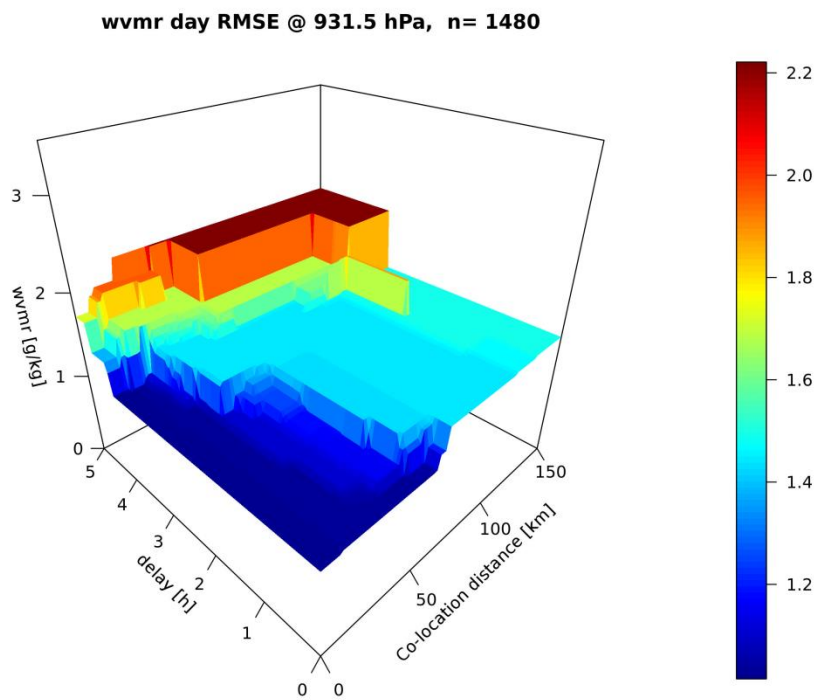


Figure 13: Net co-location uncertainty for WVMR, daytime, at 931.5 hPa.



---

### ***Applicability***

The estimates reported in the LUT's have been obtained using RAOB-IASI data in central Europe, year 2015, using the algorithm described in Section 3.2. Assuming stationarity over time and in the climatic region, it can be extended to neighboring years and the GRUAN station of Sodankyla.

Hence these LUT's may be used for the following GRUAN stations: Cabauw, Lindenberg, Payerne and Sodankyla, years 2014-2016.

The use of these LUT's in other regions and/or other periods is not recommended nor tested presently. Further work would be required prior to such an application.

## **3.4. Data access**

The high-level access point for this data set, both data file and user manual, is:

[ftp://ftp-ae.oma.be/dist/GAIA-CLIM/D3\\_6/TempHum/UniBergamo/](ftp://ftp-ae.oma.be/dist/GAIA-CLIM/D3_6/TempHum/UniBergamo/)

## 4. Library of AOD spatial and temporal mismatch uncertainties (FMI)

### 4.1. Objectives and methodology

In validation of satellite Aerosol Optical Depth (AOD) data against the Aerosol RObotic NETwork (AERONET) it is typical to use averaged values in the comparison (instead of the closest single observations) due to representativeness issues between the point-like AERONET observations and the satellite observations covering a larger sampling area. The averaging also enables the assessment of the related collocation mismatch uncertainty by statistical means, i.e. by calculating the associated standard deviations. The spatial AOD mismatch uncertainty estimate is obtained from the standard deviation of satellite AOD within the sampling area, as illustrated in Figure 14 below. The temporal mismatch uncertainty is estimated by the standard deviation of the AERONET AOD within the temporal sampling window.

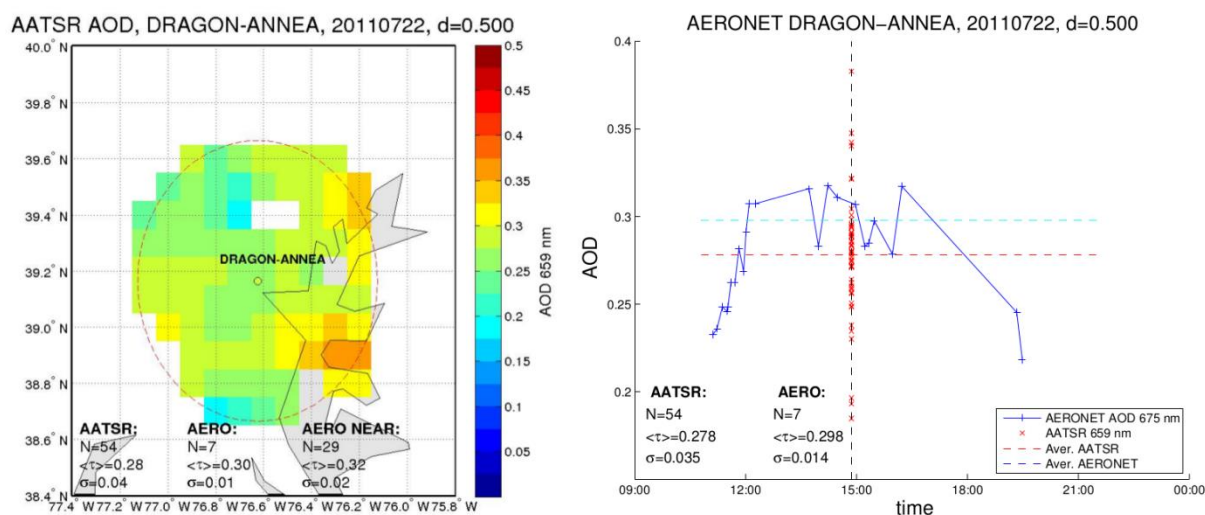


Figure 14: Illustration of the AOD comparison between AERONET and AATSR. a) The color shows the AATSR AOD values around an AERONET site. The dashed line shows the sampling area. b) The blue curve shows the AERONET observations as function of time while the red dots show the AATSR observation at the overpass. The dashed lines show the obtained average values.

The optimal sampling parameters for the validation depend on the atmospheric conditions and on the site location. Therefore the AOD uncertainty library provides the uncertainty estimates obtained with a range of sampling parameters. Although the standard deviations can be used as estimates of the collocation mismatch uncertainty between the AATSR and AERONET AOD products, it must be emphasized that in addition to the 'true' AOD variation they are affected by retrieval errors. In particular, the spatial standard deviation obtained from the AATSR data has a significant contribution from the retrieval errors, caused by e.g. surface reflectance variation and cloud contamination. For further details, we refer to GAIA-CLIM deliverable D3.4.



## 4.2. Library description and user guide

The files contain collocated AOD data from the European Space Agency's (ESA) Advanced Along Track Scanning Radiometer (AATSR) satellite instrument which flew onboard ENVISAT over 2002-2012, and from the AERONET sunphotometer network. For each AATSR orbit the AERONET database is searched for spatial and temporal matches, using a predefined sampling distance around the site for AATSR data and a predefined sampling time window centred at the overpass time for the AERONET data.

The first data set ('GLOBAL') contains data for the full AATSR mission from August 2002 to April 2012 and from nearly 900 AERONET sites (this number includes current and former sites, temporary sites, and different instrument versions of the same site). In total, there are over 63000 matches (collocated measurements) between AATSR and AERONET. The second data set ('DRAGON') contains data for the AERONET Distributed Regional Aerosol Gridded Observation Networks (DRAGON) measurements in the summer of 2011 in the greater Baltimore area (Maryland, USA). The use of this set of densely located AERONET sites allows the calculation of the spatial standard deviation of AOD from the AERONET sites with the same spatial sampling as used for the AATSR data. These data allow the evaluation of the AOD spatial mismatch uncertainty estimate (Figure 15).

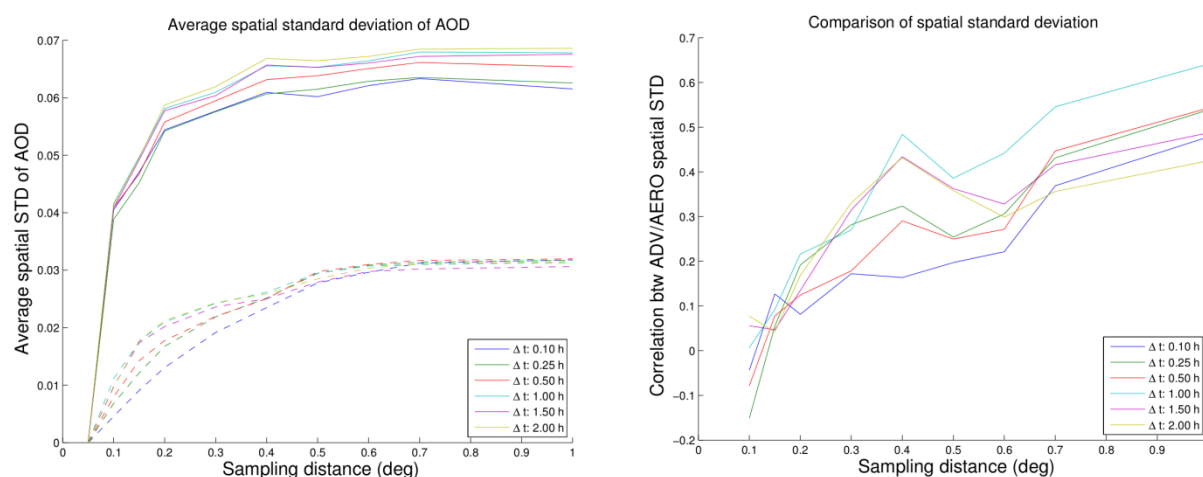


Figure 15: Left-hand panel: The spatial AOD uncertainty estimate depends on the sampling parameters. The solid lines show the average STD for AATSR, while the dashed lines correspond to AERONET DRAGON data. Right-hand panel: The correlation between the spatial AOD variability obtained from AATSR and from AERONET improves with the sampling distance.

Each spatially and temporally collocated match between AATSR and AERONET is recorded as a single datum in the database. After an initial match is identified using the largest sampling distance and sampling time gap, a list of smaller distances and time gaps is applied for calculating the spatially averaged AATSR AOD and the temporally averaged AERONET AOD. The corresponding standard deviations are also calculated.

In the Annex C, the variables included in the database are briefly described. Annex D stipulates the licensing for use of the AERONET data.



---

## 4.1. Data access

The high-level access point for this data set, both data file and user manual, is:

[ftp://ftp-ae.oma.be/dist/GAIA-CLIM/D3\\_6/AOD/FMI/](ftp://ftp-ae.oma.be/dist/GAIA-CLIM/D3_6/AOD/FMI/)



## 5. Data set of dedicated GRUAN-processed RS92 launches for co-location with IASI (FMI)

### 5.1. Objectives

The objective is to provide a specific dataset of fully traceable radiosonde temperature and humidity measurements performed at (and co-located with) IASI overpass times so as to minimize the co-location mismatch. This dataset will help illustrate the potential of dedicated ground-based campaigns.

This library consists of 350 temperature and humidity profiles measured by RS92 radiosonde during IASI/MetOp overpasses. In addition we have also included data from regular sonde launches from the same period of measurement. Thus the full data set consists of 537 files. The dedicated measurements, as well as the regular measurements were already made during the Atmospheric Sounding Campaign in summer 2007 over Sodankylä, Finland (at 67.37° N, 26.63° E), see e.g. Calbet et al. (2011), but the post-processing of the data was now done according to the GRUAN processing algorithm, which includes corrections for humidity sensor lag error and a radiation heating correction (Dirksen et al., 2014). As such, this data set now addresses both the metrological traceability of the measurements and the (temporal) co-location issue of comparisons with IASI/MetOp.

### 5.2. Methodology

The RS92 launches to measure T and q profiles were made 60 minutes and 5 minutes before each IASI overpass. The time period of the launches is from June 4 until September 5, 2007. The launch site is Sodankylä in Northern Finland (at 67.37° N, 26.63° E).

The GCOS (Global Climate Observing System) Reference Upper-Air Network (GRUAN) data processing for the Vaisala RS92 radiosonde was used to process the radiosonde data. An important aspect of the GRUAN processing is that the uncertainty estimates are vertically resolved. The algorithms correct for systematic errors in radiosonde measurements of pressure, temperature, humidity and wind, as well as how the uncertainties related to these error sources are derived.

GRUAN uncertainty estimates are 0.15 K for night-time temperature measurements and approximately 0.6 K at 25 km during daytime. The other uncertainty estimates are up to 6 %RH for humidity, 10–50 m for geopotential height, 0.6 hPa for pressure, 0.4–1 m/s for wind speed, and 1° for wind direction.



## 5.3. Data set description and user guide

The data are provided in NetCDF format. NetCDF is a self-describing binary format that was developed by UNIDATA. Software libraries for handling NetCDF files are available for a variety of programming languages at [www.unidata.ucar.edu/software/netcdf](http://www.unidata.ucar.edu/software/netcdf).

The processing uses NetCDF’s capabilities to include meta-data. The data format description is provided by Sommer et al. (2016).

Details of the sonde launches are given in Table 1 (only partially shown here, see Annex E for the complete table).

The summary includes launch times and Metop IASI overpass (OVP) times in UTC. RS92 (PTU) data coverage indicates whether or not the PTU was fully operational during sonde launch. The burst pressure, the maximum height of sonde operation, is marked red when larger than 10 hPa.” Some of the RS92 payloads included additional sensors: green color marks ozone sensors and red color and additional CFH instrument, if included in the payload.

Table 1: Summary of the GRUAN-processed dedicated RS92 sonde launches for co-location with IASI (full table in Annex E)

Date	Launch time t1	Metop OVP time t2	t2 - t1 (min)	Metop orbit numb er	Burst altitud e (km)	Burst pressu re (hPa)	Total cloudi ness (octa)	Amou nt of low clouds (octa)	PTU data coverage		
									T (%)	RH (%)	GPS (%)
04-06-07	07:08:02	08:07:57	60	3234	32.4	9.1	4	1	100.0	100.0	100.0
04-06-07	08:03:00	08:07:57	5	3234	34.2	7.0	6	1	100.0	100.0	99.5
05-06-07	16:43:17	17:43:14	60	3254	31.3	10.6	4	1	100.0	100.0	100.0
06-06-07	08:06:38	09:06:54	60	3263	33.6	7.7	8	8	100.0	100.0	100.0
06-06-07	09:01:38	09:06:54	5	3263	33.8	7.4	8	8	100.0	100.0	100.0
06-06-07	18:02:47	19:02:46	60	3269	31.9	9.8	7	5	100.0	100.0	100.0
06-06-07	18:57:47	19:02:46	5	3269	32.6	8.8	7	4	100.0	100.0	100.0
07-06-07	07:46:08	08:46:08	60	3277	32.3	9.2	1	0	100.0	100.0	100.0
07-06-07	08:41:08	08:46:08	5	3277	33.4	7.9	1	1	100.0	100.0	100.0
07-06-07	17:42:33	18:41:57	59	3283	34.0	7.3	1	1	100.0	100.0	100.0
07-06-07	18:36:55	18:41:57	5	3283	32.5	9.0	1	0	100.0	100.0	100.0
08-06-07	07:25:18	08:25:19	60	3291	33.2	8.1	7	7	100.0	100.0	100.0



---

<b>08-06-07</b>	<b>08:20:20</b>	08:25:19	5	3291	33.1	8.2	7	7	100.0	100.0	100.0
-----------------	-----------------	----------	---	------	------	-----	---	---	-------	-------	-------





---

## 6. Conclusion and prospects

This document, part of GAIA-CLIM Deliverable D3.6, describes libraries of smoothing, sampling, and co-location uncertainties constructed for temperature, humidity, total ozone column, and aerosol optical depth, for several key ground-based observing systems. Also provided is a data set of dedicated RS92 radiosonde launches, timed to coincide with IASI/MetOP overpasses, and now processed following GRUAN protocol.

Great effort has been put into providing this material to the user community in formats that are straightforward to interpret and use. In view of the exploratory nature of this work, feedback from the user community will be sought, and this will undoubtedly lead to further refinement of the libraries, part of which will occur still during the GAIA-CLIM lifetime. Such improvements will be reported on in updates of this document, available with the data files, accessible directly via ftp at [ftp://ftp-ae.oma.be/dist/GAIA-CLIM/D3\\_6](ftp://ftp-ae.oma.be/dist/GAIA-CLIM/D3_6) or (in the near future) through the WP3 page at <http://www.gaia-clim.eu>. Also an extension towards other networks, ECVs, observing techniques etc. is needed, but this is beyond the scope of GAIA-CLIM and is for that reason included in both the GAID and recommendations document.



## References and related documentation

Butterfield, D. and Gardiner, T, 2015: Determining the temporal variability in atmospheric temperature profiles measured using radiosondes and assessment of correction factors for different launch schedules; *Atmos. Meas. Tech.*, 8, 463–470.

Calbet, X., R. Kivi, S. Tjemkes, F. Montagner, R. Stuhlmann (2011), Matching radiative transfer models and radiosonde data from the EPS/Metop Sodankylä campaign to IASI measurements, *Atmos. Meas. Tech.*, 4, 1177-1189, doi:10.5194/amt-4-1177-2011.

Dirksen, R. J.; Sommer, M.; Immler, F. J.; Hurst, D. F.; Kivi, R. & Vömel, H. Reference quality upper-air measurements: GRUAN data processing for the Vaisala RS92 radiosonde *Atmos. Meas. Tech.*, 2014, 7, 4463-4490

Sommer, M., R. Dirksen and C. von Rohden [GRUAN-TD-4](#): Brief Description of the RS92 GRUAN Data Product (RS92-GDP), v2.0 (2016-02-11).

Verhoelst, T., Granville, J., Hendrick, F., Köhler, U., Lerot, C., Pommereau, J.-P., Redondas, A., Van Roozendael, M., and Lambert, J.-C.: Metrology of ground-based satellite validation: co-location mismatch and smoothing issues of total ozone comparisons, *Atmos. Meas. Tech.*, 8, 5039-5062, doi:10.5194/amt-8-5039-2015, 2015.

D3.2: Generic metrology aspects of an atmospheric composition measurement and of data comparisons. EC Horizon2020 GAIA-CLIM technical Report / Deliverable D3.2 BIRA-IASB, 2016

D3.4: Measurement mismatch studies and their impact on data comparisons. EC Horizon2020 GAIA-CLIM technical Report / Deliverable D3.4 BIRA-IASB, 2017

D3.5: Beta set of tools for quantification of collocation mismatch and smoothing uncertainties and associated documentation for integration in the development of the virtual observatory. EC Horizon2020 GAIA-CLIM technical Report / Deliverable D3.5 BIRA-IASB, 2017

D3.7: Final version of tools for quantification of collocation mismatch and smoothing uncertainties and associated documentation for integration in the development of the virtual observatory. EC Horizon2020 GAIA-CLIM technical Report / Deliverable D3.7 BIRA-IASB, 2017

## Acronyms

AATSR	Advanced Along Track Scanning Radiometer
AERONET	Aerosol Robotic Network
AMT	Atmospheric Measurement Techniques
AOD	Aerosol Optical Depth
CEU	Central Europe
ECV	Essential Climate Variable
GRUAN	Global climate observing system Reference Upper-Air Network
IASI	Infrared Atmospheric Sounding Interferometer
IR	Infra Red
LUT	Look-Up Table



---

NDACC	Network for the Detection of Atmospheric Composition Change
OSSMOSE	Observing System of Systems Simulator for Multi-mission Synergies Exploration
RAOB	RAdiosonde Observations
SAOZ	Système d'Analyse par Observation Zénithale
SZA	Solar Zenith Angle
TOC	Total Ozone Column
UV	Ultra Violet
VO	Virtual Observatory
ZSL-DOAS	Zenith-sky Scattered-Light Differential Optical Absorption Spectroscopy

## Annex A: Example total O<sub>3</sub> column information sheet



aeronomie.be

### Total O<sub>3</sub> smoothing and co-location uncertainties at Observatoire de Haute-Provence



#### 1 Purpose of this information sheet

This information sheet presents estimated smoothing and co-location errors and uncertainties for total ozone column measurements obtained with the direct-sun UV/Vis (and -if applicable- near-IR) and zenith-sky UV-Vis instrument(s) at Observatoire de Haute-Provence. The errors were estimated with the OSSSMOSE system developed at BIRA-IASB (Verhoelst et al., AMT v8, 2015). These information sheets were produced in the context of the European Commission's H2020 project GAIA-CLIM (grant nr. 640276), and further documentation can be found at [www.gaia-clim.eu](http://www.gaia-clim.eu). In particular, the user is referred to Deliverables D3.2 and D3.6, both also available for download with the netCDF data files supporting this information sheet (see Section 9).

#### 2 Station and instrument specifics

Name	Observatoire de Haute-Provence
Latitude	43.94°
Longitude	5.71°
Altitude	650m a.m.s.l.
Instruments	Dobson (Beck, nr085), SAOZ (CP200 NMOS1024, nr013), SAOZ (CP200 NMOS512, nr013)

#### 3 Smoothing uncertainty: Direct-sun measurements

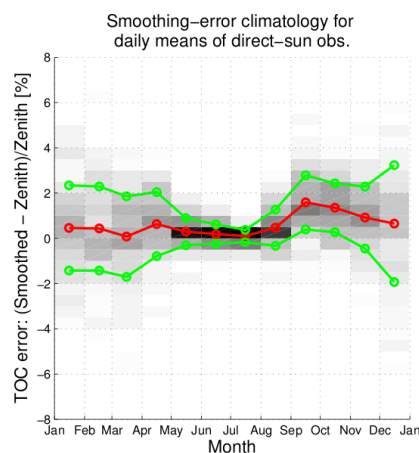


Figure 1: Horizontal smoothing errors for daily means of direct-sun measurements. The grey scale represents the density of the simulated smoothing errors, the red curve the monthly mean smoothing error (i.e. the resulting bias) and the green curves the standard deviation of the smoothing errors around the mean.





#### 4 Smoothing uncertainty: Zenith-sky measurements

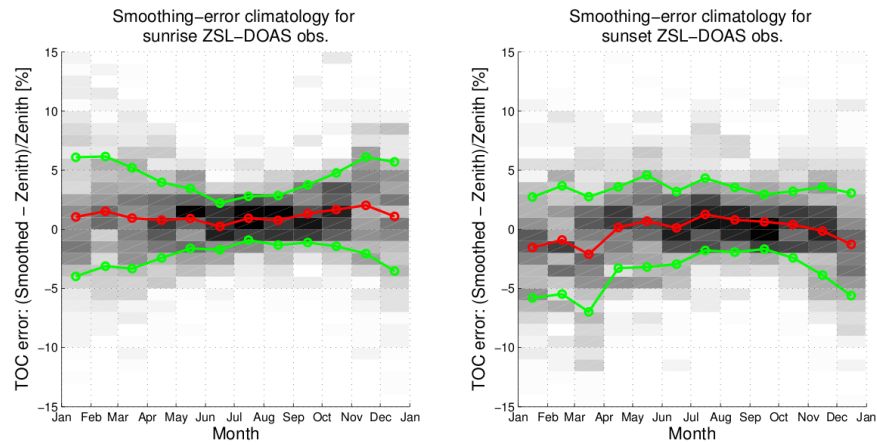


Figure 2: Horizontal smoothing errors for sunrise (left-hand panel) and sunset(right-hand panel) zenith-sky measurements. The grey scale represents the density of the simulated smoothing errors, the red curve the monthly mean smoothing error (i.e. the resulting bias) and the green curves the standard deviation of the smoothing errors around the mean.



## 5 Natural variability

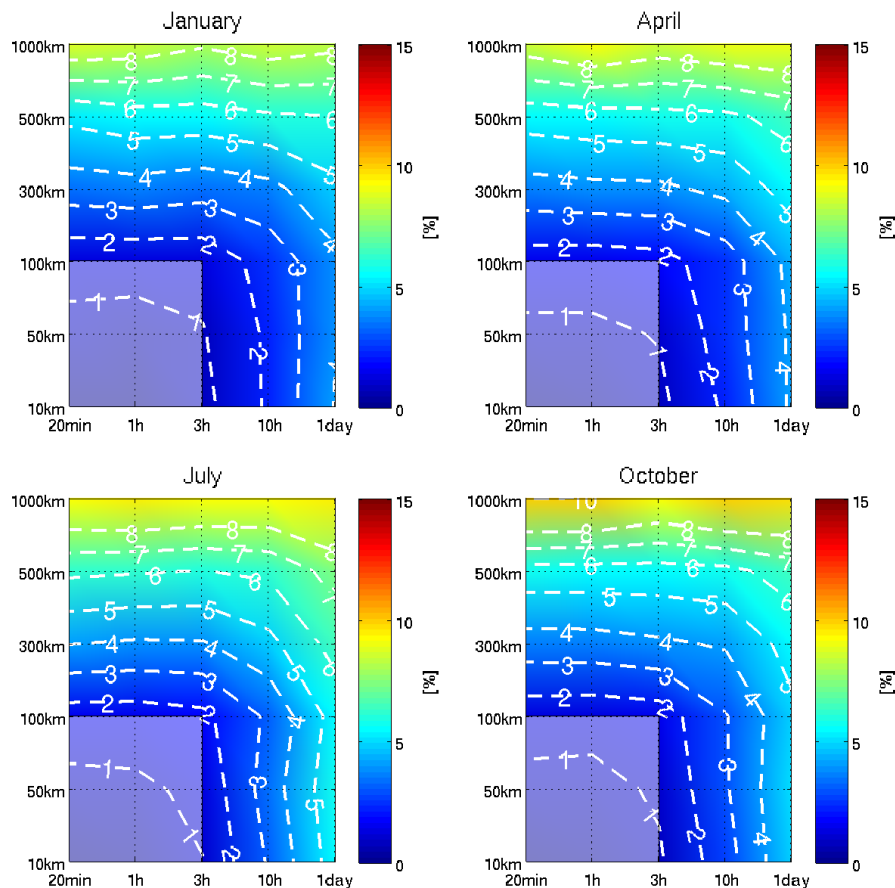


Figure 3: Natural variability (spread of the difference w.r.t. the value at the station zenith) as a function of separation in time (x-axis) and space (y-axis) for 4 months representing the different seasons. The shaded boxes in the lower left-hand corner denote the regime for which the model fields had to be oversampled (linearly). Because the systematic part is highly non-isotropic (e.g. due to North-South gradients), it can not be reported as a function of  $dr$  and  $dt$  only. It is covered in the subsequent section on co-location uncertainties.



## 6 Co-location uncertainty: Direct-sun measurements

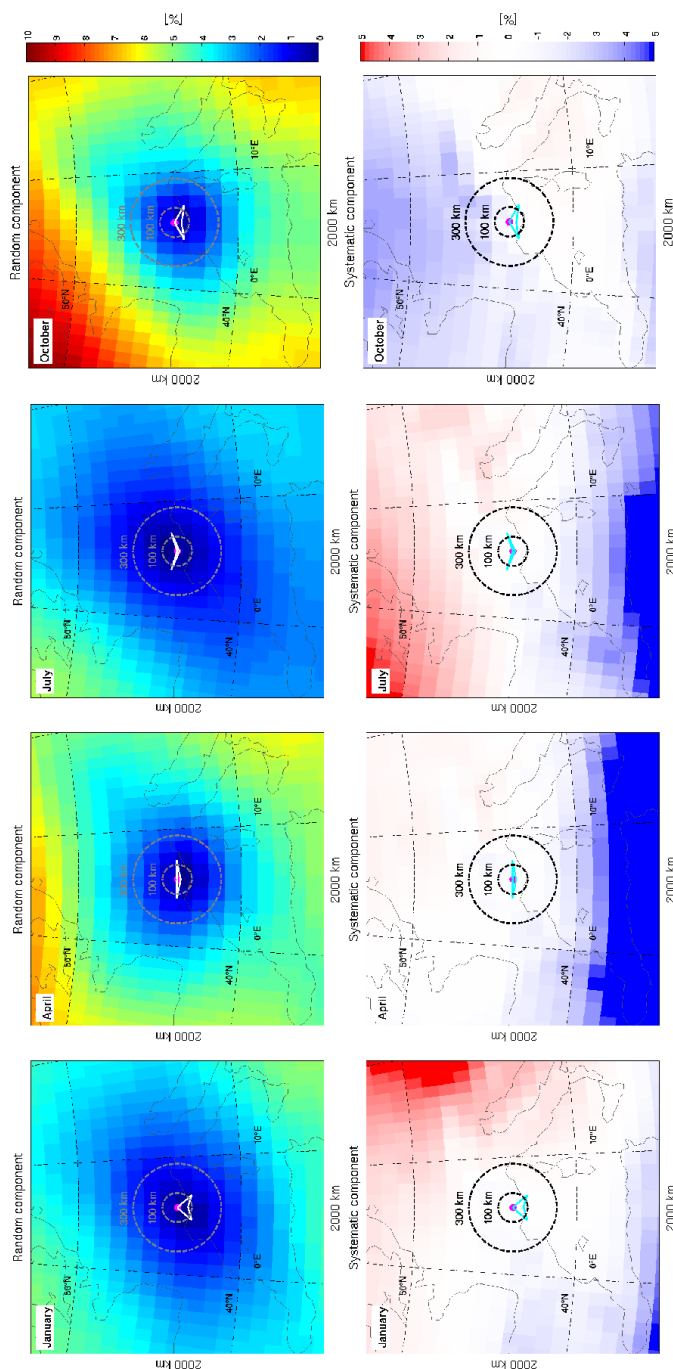


Figure 4: Full spatial co-location uncertainty estimates between the ground-based measurements and neighbouring independent measurements (e.g. from a satellite sounder), including the horizontal smoothing effect in the ground-based measurement. From left to right: 4 months representing the different seasons. Top panels: random part of the co-location uncertainty. Bottom panels: systematic part of the co-location errors. The dashed circles indicate some distances for reference. The white (upper panels) and cyan (lower panels) polygons denote the area of measurement sensitivity. The station itself is marked in magenta.

## 7 Co-location uncertainty: sunrise ZSL-DOAS

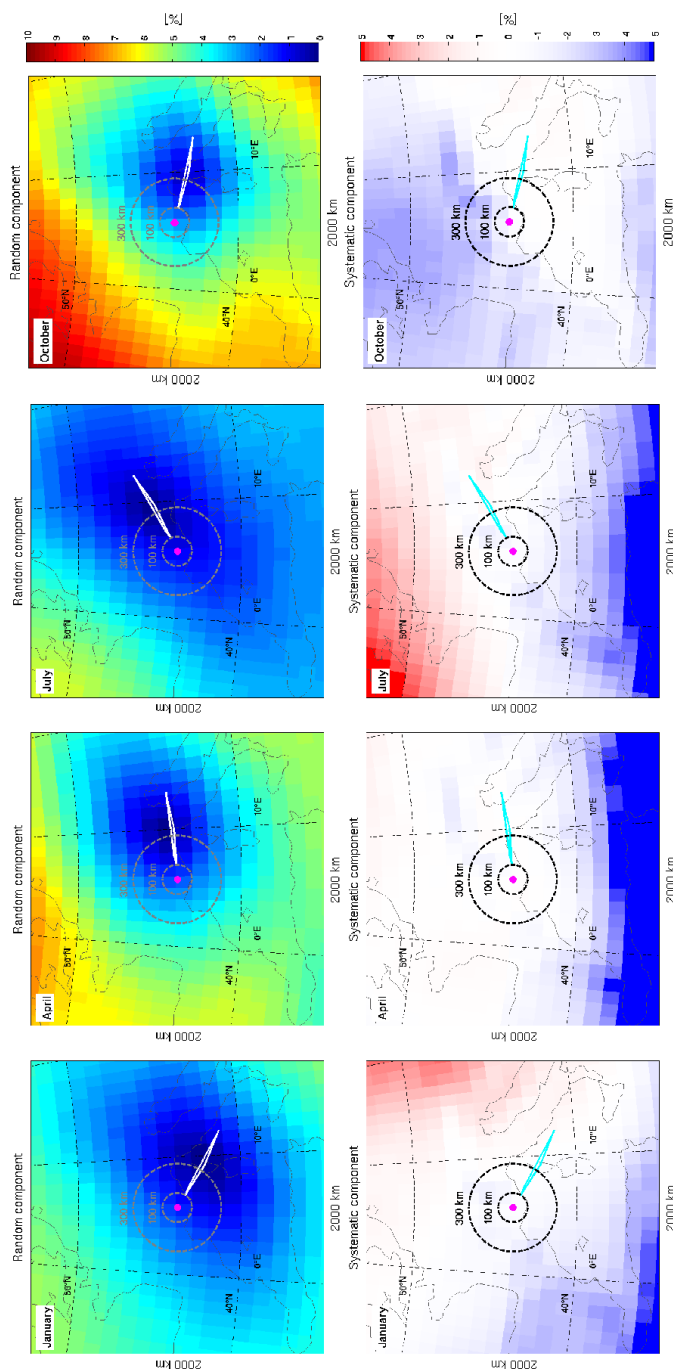


Figure 5: Full spatial co-location uncertainty estimates between the sunrise ZSL-DOAS measurements and neighbouring independent measurements (e.g. from a satellite sounder), including the horizontal smoothing effect in the ground-based measurement. From left to right: 4 months representing the different seasons. Top panels: random part of the co-location uncertainty. Bottom panels: systematic part of the co-location errors. The dashed circles indicate some distances for reference. The white (upper panels) and cyan (lower panels) polygons illustrate the area of measurement sensitivity. The station itself is marked in magenta.



## 8 Co-location uncertainty: sunset ZSL-DOAS

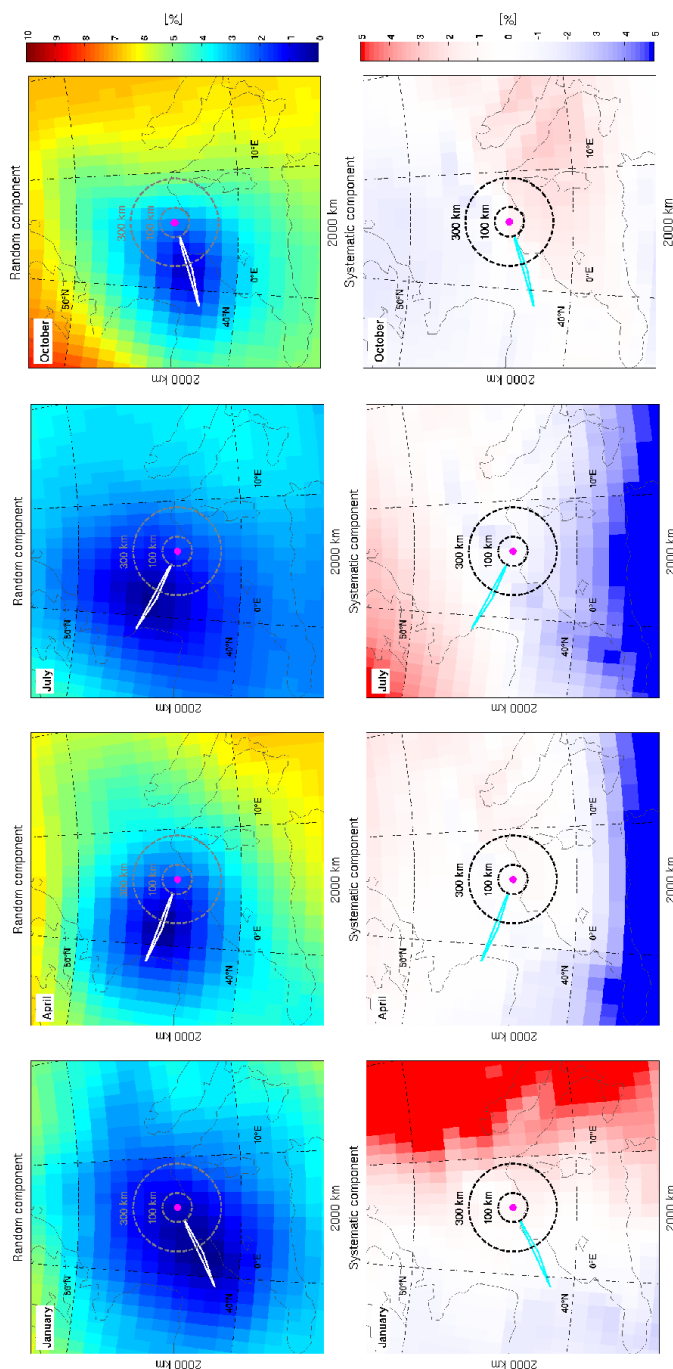


Figure 6: Full spatial co-location uncertainty estimates between the sunset ZSL-DOAS measurements and neighbouring independent measurements (e.g. from a satellite sounder), including the horizontal smoothing effect in the ground-based measurement. From left to right: 4 months representing the different seasons. Top panels: random part of the co-location uncertainty. Bottom panels: systematic part of the co-location errors. The dashed circles indicate some distances for reference. The white (upper panels) and cyan (lower panels) polygons illustrate the area of measurement sensitivity. The station itself is marked in magenta.



aeronomie.be

## Total O<sub>3</sub> smoothing and co-location uncertainties at Observatoire de Haute-Provence



### 9 Data access and permissions

The data presented here can be obtained as netCDF files via anonymous ftp at <ftp://ftp-ae.oma.be/dist/GAIA-CLIM/D3.6/Ozone/BIRA/netCDF/ohp/>. Specifically, the following files are available:

- *SmoothingErrors/TOC\_ohp\_sunrise\_ZSL-DOAS\_SmoothingErrors.nc*
- *SmoothingErrors/TOC\_ohp\_sunset\_ZSL-DOAS\_SmoothingErrors.nc*
- *SmoothingErrors/TOC\_ohp\_daily-mean\_direct-sun\_SmoothingErrors.nc*
- *NatVar/TOC\_ohp\_NaturalVariability.nc*
- *CoLocation/TOC\_ohp\_sunrise\_ZSL-DOAS\_CoLocationUncertainty.nc*
- *CoLocation/TOC\_ohp\_sunset\_ZSL-DOAS\_CoLocationUncertainty.nc*
- *CoLocation/TOC\_ohp\_daily-mean\_direct-sun\_CoLocationUncertainty.nc*

Before use in publications or commercial applications, please contact [tijl.verhoelst@aeronomie.be](mailto:tijl.verhoelst@aeronomie.be) to discuss appropriate acknowledgments.

#### Revision history

Issue	Rev.	Date	Section	Description of Change
1	A	31/08/2017	all	Creation of this information sheet





## Annex B: File description for "D3.6\_IASI-RAOB\_Uncertainty\_v2.h5"

File type: Hierarchical Data Format, version 5

```
group: Temperature {
  group: Day {
    variables:
      double colocDistance(101);
      :Descr = "IASI-sonde distance";
      :Units = "Km";
      :_ChunkSizes = 101; // int
      double colocTimeDifference(101);
      :Descr = "IASI-sonde time difference (absolute value)";
      :Units = "hours";
      :_ChunkSizes = 101; // int
      double colocUncertainty(75, 101, 101);
      :Units = "K";
      :Descr = "Temperature Colocation uncertainty";
      :DimDescr = "pressure level x distance x time difference";
      :Algorithm = "GAIA-CLIM Deliverable D3.4 Sect. 3 and Annex 1 to D3.6 ";
      :Applicability = "GRUAN stations Sodankylä, Lindenberg, Cabaw, Payerne, year 2015";
      :_ChunkSizes = 75, 101, 101; // int
      double pressureLevel(75);
      :Descr = "IASI pressure levels";
      :Units = "hPa";
      :_ChunkSizes = 75; // int

      // group attributes:
      :Definition = "Day is ground level colocation time between 4:00am and 10:00pm";
  }

  group: Night {
    variables: same as group Day
    .....

    // group attributes:
    :Definition = "Night is Ground level colocation time between 4:00am and 10:00pm";
  }

  group: VerticalSmoothing {
    variables:
      double VSmoothingUncertainty(75);
      :Descr = "Vertical Smoothing uncertainty";
      :DimDescr = "pressure level";
      :Algorithm = "GAIA-CLIM Deliverable D3.4 Sect. 3 and Annex 1 to D3.6 ";
      :Applicability = "GRUAN stations Sodankylä, Lindenberg, Cabaw, Payerne, year 2015";
      :Units = "K";
      :_ChunkSizes = 75; // int
      double pressureLevel(75);
      :Descr = "IASI pressure levels";
      :Units = "hPa";
```



```

        :_ChunkSizes = 75; // int
    }
}

group: wvmr {
    group: Day {
        variables:
            double colocDistance(101);
            :Descr = "IASI-sonde distance";
            :Units = "Km";
            :_ChunkSizes = 101; // int
            double colocTimeDifference(101);
            :Descr = "IASI-sonde time difference (absolute value)";
            :Units = "hours";
            :_ChunkSizes = 101; // int
            double colocUncertainty(33, 101, 101);
            :Units = "g/Kg";
            :Descr = "WVMR Colocation uncertainty";
            :DimDescr = "pressure level x distance x time difference";
            :Algorithm = "GAIA-CLIM Deliverable D3.4 Sect. 3 and Annex 1 to D3.6 ";
            :Applicability = "GRUAN stations Sodankyhla, Lindenberg, Cabaw, Payerne, year 2015";
            :_ChunkSizes = 33, 101, 101; // int
            double pressureLevel(33);
            :Descr = "IASI pressure levels";
            :Units = "hPa";
            :_ChunkSizes = 33; // int
            // group attributes:
            :Definition = "Day is ground level colocation time between 4:00am and 10:00pm";
        }
        group: Night {
            group: Night {
                variables: same as group Day
                .....
                // group attributes:
                :Definition = "Night is Ground level colocation time between 4:00am and 10:00pm";
            }
        }
        group: VerticalSmoothing {
            variables:
            double VSmoothingUncertainty(33);
            :Descr = "Vertical Smoothing uncertainty";
            :DimDescr = "pressure level";
            :Algorithm = "GAIA-CLIM Deliverable D3.4 Sect. 3 and Annex 1 to D3.6 ";
            :Applicability = "GRUAN stations Sodankyhla, Lindenberg, Cabaw, Payerne, year 2015";
            :Units = "g/Kg";
            :_ChunkSizes = 33; // int
            double pressureLevel(33);
            :Descr = "IASI pressure levels";
            :Units = "hPa";
            :_ChunkSizes = 33; // int
        }
    }
}

```



## **Annex C:** File description for “aerosol\_uncertainty\_library\_AERONET\_AATSR\_\*.nc”

File type is netCDF.

Variables 1-12 have one value for each match.

Variables 13-24 have separate values for each time gap value in the timegap\_list. If there are no AERONET observations for a smaller time gap, a fill value is given (NaN).

Variables 25-44 have separate values for each sampling distance in the dist\_list. If there are no AATSR pixels for a smaller sampling distance, a fill value is given (NaN).

Variables 45-47 are only available for the 'DRAGON' dataset. They have separate values for each distance and each timegap. If there is no nearby data, a fill value is given (NaN).

### **Variables:**

#### 1) dist\_list

List of sampling distances used for averaging the AATSR data around the AERONET site. The sampling area is a circle centred at the AERONET site, with the radius given by the sampling distance. The largest distance is used to determine if there is a spatial match between an AERONET site and an AATSR orbit.

#### 2) timegap\_list

List of sampling time gaps used for averaging the AERONET observations around the AATSR overpass time. Temporal sampling is applied so that the observations ( $t$ ) within  $|t_{\text{overpass}} - t| < \text{time gap}$  are accepted, i.e. a 0.5 h time gap corresponds to a one hour time window centred at the overpass time. The largest time gap is used to determine if there is a temporal match between an AERONET site and an AATSR orbit.

#### 3) site\_index

An integer index for the AERONET site, uniquely identifying the site.

#### 4) site\_name

The name of the AERONET site.

#### 5) lat

Latitude (degree north) of the AERONET site.

#### 6) lon

Longitude (degree east) of the AERONET site.

#### 7) mu\_N

Satellite zenith angle for the AATSR nadir view.



8) mu\_NO

Solar zenith angle for the AATSR nadir view.

9) mu\_F

Satellite zenith angle for the AATSR forward view.

10) mu\_F0

Solar zenith angle for the AATSR forward view. This should be (nearly) the same as mu\_NO, since the time difference between the forward and nadir is small (~2 min).

11) phi\_N

Relative azimuth angle between sun and satellite, nadir view.

12) time

Satellite overpass time, days since 0000.00.00 00:00. For example for 2000.1.1 00:00 the 'time' variable is 730486.

13) aod\_aero\_440

AERONET aerosol optical depth at 440 nm, averaged over the time window. A separate value is given for each time window size.

14) aod\_aero\_675

AERONET aerosol optical depth at 675 nm, averaged over the time window. A separate value is given for each time window size.

15) aod\_aero\_870

AERONET aerosol optical depth at 870 nm, averaged over the time window. A separate value is given for each time window size.

16) aod\_aero\_1020

AERONET aerosol optical depth at 1020 nm, averaged over the time window. A separate value is given for each time window size.

17) aod\_aero\_555

AERONET aerosol optical depth at 555 nm, averaged over the time window. Since AOD at 555 nm is not available from AERONET, this value is derived from the AERONET AOD at 440 nm using the Ångström exponent:  $Aero_{555} = \exp(\log(Aero_{440}) - \log(555/440) * Aero_{ang})$ ; A separate value is given for each time window size. Note: a negative AOD value at 440 nm (unphysical) will lead to a complex derived AOD value at 555 nm.

18) aod\_aero\_659



AERONET aerosol optical depth at 659 nm, averaged over the time window. Since AOD at 659 nm is not available from AERONET, this value is derived from the AERONET AOD at 440 nm using the Ångström exponent:  $\text{Aero}_{555} = \exp(\log(\text{Aero}_{440}) - \log(659/440) * \text{Aero}_{\text{ang}})$ ; A separate value is given for each time window size.

19) aero\_ang

AERONET Ångström exponent.

20) std\_aero\_440

Standard deviation of AOD at 440 nm within the temporal sampling window. A separate value is given for each time window size.

21) std\_aero\_675

Standard deviation of AOD at 675 nm within the temporal sampling window. A separate value is given for each time window size.

22) std\_aero\_870

Standard deviation of AOD at 870 nm within the temporal sampling window. A separate value is given for each time window size.

23) std\_aero\_1020

Standard deviation of AOD at 1020 nm within the temporal sampling window. A separate value is given for each time window size.

24) aero\_num

Number of AERONET observations within the temporal sampling window. A separate value is given for each time window size.

25) aod\_adv\_555

AATSR aerosol optical depth at 555 nm, averaged over the sampling area. A separate value is given for each sampling distance.

26) aod\_adv\_659

AATSR aerosol optical depth at 659 nm, averaged over the sampling area. A separate value is given for each sampling distance.

27) aod\_adv\_1610

AATSR aerosol optical depth at 1610 nm, averaged over the sampling area. A separate value is given for each sampling distance.

28) std\_adv\_555



Standard deviation of AOD at 555 nm within the sampling area. A separate value is given for each sampling distance.

29) std\_adv\_659

Standard deviation of AOD at 659 nm within the sampling area. A separate value is given for each sampling distance.

30) std\_adv\_1610

Standard deviation of AOD at 1610 nm within the sampling area. A separate value is given for each sampling distance.

31) adv\_num

Number of AATSR data points (pixels) within the sampling area. A separate value is given for each sampling distance.

32) adv\_ang

AATSR Ångström exponent determined from AOD at 555 and 659 nm:  $AATSR\_ang = \log(AATSR\_555/AATSR\_659)/\log(659/555)$  Averaged over the sampling area; separate value for each distance.

33) landsea

AATSR land/sea flag (0: ocean, 1: land), averaged over the sampling area. Due to the averaging, this variable gives the fraction of land pixels. Averaged over the sampling area; separate value for each distance.

34) quality

An ADV/ASV quality flag, based on the the variance of top of atmosphere (TOA) reflectance at 555 nm within one 10\*10 km retrieval area. Higher value indicates higher variance and higher uncertainty in AOD. Averaged over the sampling area; separate value for each distance.

35) RNTOA1600

Average nadir TOA reflectance at 1610 nm for one AATSR 10\*10 km pixel, used for detecting bright surfaces for which ADV performs poorly. Averaged over the sampling area; separate value for each distance.

36) kratio

Fraction between nadir and forward surface reflectance (assumed wavelength independent), used in ADV retrieval. Averaged over the sampling area; separate value for each distance.

37) adv\_nad\_surf\_refl555





AATSR surface reflectance at 555 nm, nadir view. Derived from TOA reflectance and AOD. Averaged over the sampling area. A separate value is given for each sampling distance.

38) adv\_nad\_surf\_refl659

AATSR surface reflectance at 659 nm, nadir view. Averaged over the sampling area; separate value for each distance.

39) adv\_nad\_surf\_refl1610

AATSR surface reflectance at 1610 nm, nadir view. Averaged over the sampling area; separate value for each distance.

40) adv\_uncert555

Uncertainty estimate for the AATSR AOD at 555 nm, based on the propagation of instrument uncertainty through the retrieval. Averaged over the sampling area; separate value for each distance.

41) adv\_uncert659

Uncertainty estimate for the AATSR AOD at 659 nm. Averaged over the sampling area; separate value for each distance.

42) adv\_uncert1610

Uncertainty estimate for the AATSR AOD at 1610 nm. Averaged over the sampling area; separate value for each distance.

43) adv\_finefrac

Fraction of fine mode aerosol type in the retrieved ADV aerosol model. Averaged over the sampling area; separate value for each distance.

44) adv\_finemix

Fraction of weakly absorbing particles within the fine mode part. Averaged over the sampling area; separate value for each distance.

45) aod\_near\_555

Average AERONET AOD at 555 nm from the 'nearby sites' within the sampling distance. The AERONET AOD values are first averaged over the temporal sampling window for each site, respectively. The AOD from the 'original site' in the center of the sampling area is not taken into account in the average. A separate value is given for each sampling distance and for each time gap.

46) std\_near\_555

Standard deviation of the AERONET AOD values at 555 nm from the 'nearby sites' within the sampling distance. The AERONET AOD values are first averaged over the temporal sampling



window for each site, respectively. The AOD from the 'original site' in the center of the sampling area is not taken into account in the standard deviation. A separate value is given for each sampling distance and for each time gap.

#### 47) near\_num

The number of nearby AERONET sites with (near)simultaneous data. A separate value is given for each sampling distance and for each timegap.

## **Annex D:** Licensing for use of the AERONET data

Please consider the following usage guidelines:

[https://aeronet.gsfc.nasa.gov/new\\_web/data\\_usage.html](https://aeronet.gsfc.nasa.gov/new_web/data_usage.html)

Each site has a Principal Investigator(s) (PI), responsible for deployment, maintenance and data collection. The PI has priority use of the data collected at the site. The PI is entitled to be informed of any other use of that site data. PI contact information can be found on data charts and in downloaded data files for each AERONET site.

Recommended guidelines for data use and publication: Although journal paper authorship and acknowledgement is the domain of the senior author and no policy is universally applicable, the AERONET contributors ask that every practical attempt be made to honor the following general guidelines.

Using AERONET data: Please consult with the PI(s) of the data to be used.

Referencing: Always reference the appropriate key AERONET papers for any publications.

Publishing AERONET data from a 'few' sites: Please consider authorship for the PI(s) and/or the following acknowledgement:

*We thank the (Project/PI) for (its/theirs) effort in establishing and maintaining (site name(s)) sites.*

Publishing data from 'many' sites: A general acknowledgement is typically sufficient and may read:

*We thank the (PI investigators) and their staff for establishing and maintaining the (#)sites used in this investigation.*

However if the AERONET data are a principal component of the paper then co-authorship to PI's should be offered.



## Annex E: Full list of GRUAN-processed RS92 launches for co-location with IASI

Date	Launch time t1	Metop OVP time t2	t2 - t1 (min)	Metop orbit numb er	Burst altitud e (km)	Burst pressu re (hPa)	Total cloudi ness (octa)	Amou nt of low clouds (octa)	PTU data coverage		
									T (%)	RH (%)	GPS (%)
04-06-07	07:08:02	08:07:57	60	3234	32.4	9.1	4	1	100.0	100.0	100.0
04-06-07	08:03:00	08:07:57	5	3234	34.2	7.0	6	1	100.0	100.0	99.5
05-06-07	16:43:17	17:43:14	60	3254	31.3	10.6	4	1	100.0	100.0	100.0
06-06-07	08:06:38	09:06:54	60	3263	33.6	7.7	8	8	100.0	100.0	100.0
06-06-07	09:01:38	09:06:54	5	3263	33.8	7.4	8	8	100.0	100.0	100.0
06-06-07	18:02:47	19:02:46	60	3269	31.9	9.8	7	5	100.0	100.0	100.0
06-06-07	18:57:47	19:02:46	5	3269	32.6	8.8	7	4	100.0	100.0	100.0
07-06-07	07:46:08	08:46:08	60	3277	32.3	9.2	1	0	100.0	100.0	100.0
07-06-07	08:41:08	08:46:08	5	3277	33.4	7.9	1	1	100.0	100.0	100.0
07-06-07	17:42:33	18:41:57	59	3283	34.0	7.3	1	1	100.0	100.0	100.0
07-06-07	18:36:55	18:41:57	5	3283	32.5	9.0	1	0	100.0	100.0	100.0
08-06-07	07:25:18	08:25:19	60	3291	33.2	8.1	7	7	100.0	100.0	100.0
08-06-07	08:20:20	08:25:19	5	3291	33.1	8.2	7	7	100.0	100.0	100.0
08-06-07	17:21:28	18:21:11	60	3297	34.4	6.8	7	6	100.0	100.0	100.0
08-06-07	18:16:19	18:21:11	5	3297	28.5	15.9	7	6	100.0	100.0	100.0
09-06-07	08:45:49	09:44:51	59	3306	33.3	8.0	7	7	100.0	100.0	100.0
09-06-07	09:42:25	09:44:51	2	3306	33.9	7.4	6	4	100.0	100.0	100.0
09-06-07	17:00:24	18:00:28	60	3311	35.4	6.0	7	3	100.0	100.0	100.0
09-06-07	17:55:25	18:00:28	5	3311	34.8	6.5	6	1	100.0	100.0	100.0
10-06-07	08:26:35	09:24:10	58	3320	35.3	6.1	3	2	100.0	100.0	100.0
10-06-07	09:20:47	09:24:10	3	3320	35.4	6.0	2	1	100.0	100.0	100.0
10-06-07	16:39:43	17:39:47	60	3325	35.3	6.1	2	2	100.0	100.0	100.0
10-06-07	17:34:43	17:39:47	5	3325	33.4	7.9	4	1	100.0	100.0	100.0



12-06-07	09:22:41	10:22:41	60	3349	34.8	6.6	8	7	100.0	100.0	100.0
12-06-07	10:17:41	10:22:41	5	3349	35.1	6.3	8	7	100.0	100.0	100.0
12-06-07	17:38:30	18:38:29	60	3354	31.8	9.9	6	4	100.0	100.0	100.0
12-06-07	18:33:21	18:38:29	5	3354	33.2	8.1	6	5	100.0	100.0	100.0
13-06-07	09:02:05	10:02:04	60	3363	32.3	9.3	8	8	100.0	100.0	100.0
13-06-07	09:57:04	10:02:04	5	3363	33.6	7.7	8	8	100.0	100.0	100.0
15-06-07	08:21:42	09:20:42	59	3391	32.5	9.0	7	6	100.0	100.0	100.0
15-06-07	09:15:43	09:20:42	5	3391	34.0	7.4	6	4	100.0	100.0	100.0
15-06-07	16:36:20	17:36:20	60	3396	34.0	7.4	7	5	100.0	100.0	100.0
15-06-07	17:31:20	17:36:20	5	3396	35.0	6.5	7	6	100.0	100.0	100.0
16-06-07	08:01:32	08:59:58	58	3405	32.6	9.0	7	7	100.0	100.0	100.0
16-06-07	08:54:56	08:59:58	5	3405	33.6	7.8	7	7	100.0	100.0	100.0
16-06-07	17:55:49	18:55:48	60	3411	35.4	6.1	8	3	100.0	100.0	100.0
16-06-07	18:50:49	18:55:48	5	3411	34.9	6.6	8	6	100.0	100.0	100.0
17-06-07	07:39:12	08:39:11	60	3419	34.6	6.8	7	7	100.0	100.0	100.0
17-06-07	08:34:11	08:39:11	5	3419	35.4	6.1	7	7	100.0	100.0	100.0
17-06-07	17:35:01	18:35:01	60	3425	34.2	7.2	7	2	100.0	100.0	100.0
17-06-07	18:30:02	18:35:01	5	3425	35.1	6.3	7	1	100.0	100.0	100.0
18-06-07	08:59:52	09:58:37	59	3434	33.0	8.6	7	5	100.0	100.0	100.0
18-06-07	09:53:39	09:58:37	5	3434	33.1	8.4	7	6	100.0	100.0	100.0
18-06-07	17:14:15	18:14:16	60	3439	34.6	6.8	5	3	100.0	100.0	100.0
18-06-07	18:09:15	18:14:16	5	3439	34.6	6.9	7	3	100.0	100.0	100.0
19-06-07	08:37:57	09:37:57	60	3448	32.8	8.8	7	5	100.0	100.0	100.0
19-06-07	09:32:56	09:37:57	5	3448	34.8	6.7	6	5	100.0	100.0	100.0
19-06-07	16:53:31	17:53:33	60	3453	35.0	6.5	6	5	100.0	100.0	100.0
19-06-07	17:48:42	17:53:33	5	3453	32.5	9.2	6	5	100.0	100.0	100.0
20-06-07	08:17:14	09:17:14	60	3462	33.0	8.5	8	7	100.0	100.0	100.0
20-06-07	09:12:14	09:17:14	5	3462	34.8	6.6	7	7	100.0	100.0	100.0
20-06-07	16:32:44	17:32:53	60	3467	34.5	6.9	6	5	100.0	100.0	100.0
20-06-07	17:27:30	17:32:53	5	3467	34.0	7.4	7	6	100.0	100.0	100.0



21-06-07	07:56:30	08:56:30	60	3476	34.7	6.7	7	7	100.0	100.0	100.0
21-06-07	08:51:30	08:56:30	5	3476	35.7	5.9	7	7	100.0	100.0	100.0
21-06-07	17:52:19	18:52:20	60	3482	33.3	8.2	3	1	100.0	100.0	100.0
21-06-07	18:47:19	18:52:20	5	3482	34.2	7.3	2	1	100.0	100.0	100.0
22-06-07	07:35:43	08:35:42	60	3490	31.3	10.9	2	2	100.0	100.0	100.0
22-06-07	08:30:42	08:35:42	5	3490	33.7	7.8	2	2	100.0	100.0	100.0
22-06-07	17:31:31	18:31:32	60	3496	34.1	7.4	1	1	100.0	100.0	100.0
22-06-07	18:26:32	18:31:32	5	3496	33.6	7.9	1	0	100.0	100.0	100.0
23-06-07	08:55:10	09:55:10	60	3505	33.6	7.8	7	4	100.0	100.0	100.0
23-06-07	09:50:09	09:55:10	5	3505	34.3	7.2	7	4	100.0	100.0	100.0
23-06-07	17:10:47	18:10:48	60	3510	33.5	8.0	3	1	100.0	100.0	100.0
23-06-07	18:05:48	18:10:48	5	3510	17.8	80.6	3	1	100.0	100.0	100.0
24-06-07	08:34:28	09:34:29	60	3519	34.2	7.3	6	2	100.0	100.0	100.0
24-06-07	09:29:29	09:34:29	5	3519	33.7	7.9	7	2	100.0	100.0	100.0
24-06-07	16:50:07	17:50:06	60	3524	34.6	6.9	7	2	100.0	100.0	100.0
24-06-07	17:45:08	17:50:06	5	3524	34.6	6.9	7	2	100.0	100.0	100.0
25-06-07	08:13:44	09:13:46	60	3533	33.3	8.2	8	8	100.0	100.0	100.0
25-06-07	09:08:52	09:13:46	5	3533	35.7	5.9	8	7	100.0	100.0	100.0
25-06-07	16:29:26	17:29:26	60	3538	34.5	7.0	8	8	100.0	100.0	100.0
25-06-07	17:24:25	17:29:26	5	3538	35.1	6.5	8	8	100.0	100.0	100.0
26-06-07	07:53:00	08:53:01	60	3547	35.6	6.0	8	8	100.0	100.0	100.0
26-06-07	08:49:21	08:53:01	4	3547	33.4	8.0	7	7	100.0	100.0	100.0
26-06-07	17:48:49	18:48:51	60	3553	34.5	6.9	7	5	100.0	100.0	100.0
26-06-07	18:43:50	18:48:51	5	3553	33.0	8.6	7	1	100.0	100.0	100.0
27-06-07	07:32:12	08:32:13	60	3561	32.8	8.8	7	7	100.0	100.0	100.0
27-06-07	08:27:12	08:32:13	5	3561	35.0	6.5	7	6	100.0	100.0	100.0
27-06-07	17:28:13	18:28:04	60	3567	33.8	7.7	6	6	100.0	100.0	100.0
27-06-07	18:23:20	18:28:04	5	3567	35.1	6.5	7	7	100.0	100.0	100.0
28-06-07	08:51:42	09:51:42	60	3576	36.2	5.6	7	5	100.0	100.0	100.0
28-06-07	09:46:43	09:51:42	5	3576	35.7	6.0	7	6	100.0	100.0	100.0



28-06-07	17:07:44	18:07:20	60	3581	34.3	7.2	7	3	100.0	100.0	100.0
28-06-07	18:02:21	18:07:20	5	3581	33.6	7.9	7	4	100.0	78.5	92.9
29-06-07	08:31:14	09:31:02	60	3590	32.3	9.5	7	3	100.0	100.0	100.0
29-06-07	09:28:43	09:31:02	2	3590	35.6	6.1	7	5	100.0	100.0	100.0
29-06-07	16:46:40	17:46:38	60	3595	33.2	8.4	7	3	100.0	100.0	100.0
29-06-07	17:41:37	17:46:38	5	3595	35.0	6.6	7	4	100.0	100.0	100.0
30-06-07	08:10:03	09:10:18	60	3604	34.7	6.9	7	5	100.0	100.0	100.0
30-06-07	09:05:12	09:10:18	5	3604	35.3	6.3	7	7	100.0	100.0	100.0
30-06-07	18:06:09	19:06:11	60	3610	35.1	6.5	8	8	100.0	100.0	100.0
30-06-07	19:01:11	19:06:11	5	3610	36.1	5.6	8	8	100.0	100.0	100.0
01-07-07	07:49:33	08:49:33	60	3618	33.4	8.2	8	8	100.0	100.0	100.0
01-07-07	08:44:33	08:49:33	5	3618	34.0	7.5	8	8	100.0	100.0	100.0
01-07-07	17:45:08	18:45:22	60	3624	32.9	8.8	7	7	100.0	100.0	100.0
01-07-07	18:40:18	18:45:22	5	3624	35.1	6.5	7	7	100.0	100.0	100.0
02-07-07	07:28:44	08:28:44	60	3632	31.8	10.2	7	7	100.0	100.0	100.0
02-07-07	08:23:44	08:28:44	5	3632	35.0	6.6	7	7	100.0	100.0	100.0
03-07-07	08:48:50	09:48:15	59	3647	34.5	7.0	7	6	100.0	100.0	100.0
03-07-07	09:43:20	09:48:15	5	3647	35.5	6.1	7	6	100.0	100.0	100.0
03-07-07	17:03:53	18:03:52	60	3652	33.3	8.3	2	2	100.0	100.0	100.0
03-07-07	17:58:52	18:03:52	5	3652	33.6	8.0	1	1	100.0	100.0	100.0
04-07-07	08:27:55	09:27:34	60	3661	31.8	10.3	1	0	100.0	100.0	100.0
04-07-07	09:22:12	09:27:34	5	3661	33.8	7.7	1	0	100.0	100.0	100.0
04-07-07	16:43:10	17:43:10	60	3666	33.6	8.0	6	4	100.0	100.0	100.0
04-07-07	17:38:09	17:43:10	5	3666	33.2	8.5	7	3	100.0	100.0	100.0
05-07-07	08:06:47	09:06:50	60	3675	34.3	7.2	4	1	100.0	100.0	100.0
05-07-07	09:01:51	09:06:50	5	3675	33.9	7.7	2	2	100.0	100.0	100.0
05-07-07	18:02:27	19:02:42	60	3681	33.6	8.0	7	1	100.0	100.0	100.0
05-07-07	18:57:40	19:02:42	5	3681	31.3	11.0	4	1	100.0	100.0	100.0
06-07-07	07:46:03	08:46:04	60	3689	32.6	9.1	6	1	100.0	100.0	100.0
06-07-07	08:41:03	08:46:04	5	3689	35.2	6.4	6	1	100.0	100.0	100.0



06-07-07	17:41:57	18:41:53	60	3695	33.9	7.6	8	6	100.0	100.0	100.0
06-07-07	18:36:56	18:41:53	5	3695	33.1	8.5	8	7	100.0	100.0	100.0
07-07-07	07:25:14	08:25:15	60	3703	33.6	7.9	8	6	100.0	100.0	100.0
07-07-07	08:20:13	08:25:15	5	3703	35.0	6.6	8	7	100.0	100.0	100.0
07-07-07	17:21:08	18:21:07	60	3709	37.0	5.0	8	7	100.0	100.0	100.0
07-07-07	18:16:07	18:21:07	5	3709	35.4	6.2	7	7	100.0	100.0	100.0
08-07-07	08:44:36	09:44:47	60	3718	33.6	8.0	8	7	100.0	100.0	100.0
08-07-07	09:39:36	09:44:47	5	3718	34.7	6.9	8	7	100.0	100.0	100.0
08-07-07	17:00:23	18:00:24	60	3723	35.9	5.8	8	7	100.0	100.0	100.0
08-07-07	17:55:24	18:00:24	5	3723	34.0	7.6	8	8	100.0	100.0	100.0
09-07-07	08:24:08	09:24:06	60	3732	33.3	8.3	8	8	100.0	100.0	100.0
09-07-07	09:19:06	09:24:06	5	3732	34.9	6.7	8	8	100.0	100.0	100.0
09-07-07	16:39:52	17:39:43	60	3737	35.3	6.3	8	7	100.0	100.0	100.0
09-07-07	17:34:25	17:39:43	5	3737	36.3	5.5	8	7	100.0	100.0	100.0
10-07-07	08:03:22	09:03:22	60	3746	37.6	4.7	8	8	100.0	100.0	100.0
10-07-07	08:58:22	09:03:22	5	3746	36.8	5.1	8	8	100.0	100.0	99.8
10-07-07	17:59:10	18:59:13	60	3752	34.6	6.9	8	4	100.0	100.0	100.0
10-07-07	18:54:17	18:59:13	5	3752	32.5	9.4	8	8	100.0	100.0	0.0
11-07-07	07:46:45	08:42:35	56	3760	32.2	9.7	8	8	100.0	100.0	100.0
11-07-07	08:37:55	08:42:35	5	3760	35.0	6.6	8	8	100.0	100.0	100.0
11-07-07	17:38:25	18:38:25	60	3766	34.8	6.7	6	6	100.0	100.0	100.0
11-07-07	18:33:24	18:38:25	5	3766	34.6	7.0	2	2	100.0	100.0	100.0
12-07-07	07:22:09	08:21:46	60	3774	34.8	6.8	6	5	100.0	100.0	100.0
12-07-07	08:17:10	08:21:46	5	3774	33.6	8.0	6	5	100.0	100.0	100.0
12-07-07	17:17:40	18:17:39	60	3780	32.6	9.2	7	4	100.0	100.0	100.0
12-07-07	18:12:39	18:17:39	5	3780	34.6	7.0	7	5	100.0	100.0	100.0
13-07-07	08:45:46	09:41:20	56	3789	33.2	8.4	7	3	100.0	100.0	100.0
13-07-07	09:36:20	09:41:20	5	3789	33.8	7.8	7	2	100.0	100.0	100.0
13-07-07	16:57:04	17:56:56	60	3794	32.7	9.1	7	5	100.0	100.0	100.0
13-07-07	17:51:52	17:56:56	5	3794	33.9	7.7	7	3	100.0	100.0	100.0



14-07-07	08:20:36	09:20:37	60	3803	36.0	5.7	8	7	100.0	100.0	100.0
14-07-07	09:15:36	09:20:37	5	3803	35.7	6.0	8	7	100.0	100.0	99.8
14-07-07	16:36:16	17:36:15	60	3808	35.4	6.2	8	2	100.0	100.0	100.0
14-07-07	17:31:14	17:36:15	5	3808	34.9	6.7	8	3	100.0	100.0	100.0
15-07-07	07:59:50	08:59:52	60	3817	34.9	6.7	7	7	100.0	100.0	100.0
15-07-07	08:54:30	08:59:52	5	3817	34.9	6.7	7	6	100.0	100.0	100.0
15-07-07	17:55:47	18:55:48	60	3823	35.3	6.4	7	7	100.0	100.0	100.0
15-07-07	18:50:48	18:55:48	5	3823	36.1	5.7	7	7	100.0	100.0	100.0
16-07-07	07:39:10	08:39:12	60	3831	33.0	8.7	7	4	100.0	100.0	100.0
16-07-07	08:34:12	08:39:12	5	3831	35.1	6.5	7	6	100.0	100.0	100.0
16-07-07	17:34:59	18:35:00	60	3837	34.0	7.5	7	5	100.0	100.0	100.0
16-07-07	18:30:00	18:35:00	5	3837	35.2	6.4	7	4	100.0	100.0	99.9
17-07-07	07:18:24	08:18:23	60	3845	31.5	10.8	2	2	100.0	100.0	100.0
17-07-07	08:13:18	08:18:23	5	3845	33.9	7.7	2	1	100.0	100.0	100.0
17-07-07	17:14:19	18:14:19	60	3851	33.2	8.4	4	2	100.0	100.0	100.0
17-07-07	18:09:19	18:14:19	5	3851	32.9	8.8	7	1	100.0	100.0	100.0
18-07-07	08:37:21	09:37:53	61	3860	34.2	7.3	8	7	100.0	100.0	100.0
18-07-07	09:32:33	09:37:53	5	3860	36.3	5.5	8	7	100.0	100.0	100.0
18-07-07	16:53:31	17:53:29	60	3865	33.5	8.1	7	2	100.0	100.0	100.0
18-07-07	17:48:31	17:53:29	5	3865	32.9	8.9	-999	4	100.0	100.0	100.0
19-07-07	08:17:50	09:17:11	59	3874	35.7	5.9	8	8	100.0	100.0	100.0
19-07-07	09:12:44	09:17:11	4	3874	34.8	6.7	8	7	100.0	100.0	100.0
19-07-07	16:33:00	17:32:49	60	3879	31.7	10.4	7	7	100.0	100.0	100.0
19-07-07	17:27:59	17:32:49	5	3879	32.6	9.1	7	7	100.0	100.0	100.0
20-07-07	07:56:22	08:56:26	60	3888	32.1	9.9	7	7	100.0	100.0	100.0
20-07-07	08:51:20	08:56:26	5	3888	33.8	7.8	7	7	100.0	100.0	100.0
20-07-07	17:52:16	18:52:16	60	3894	33.7	7.9	1	1	100.0	100.0	100.0
20-07-07	18:47:16	18:52:16	5	3894	34.3	7.3	1	0	100.0	100.0	100.0
21-07-07	07:35:23	08:35:39	60	3902	32.8	8.9	4	3	100.0	100.0	100.0
21-07-07	08:30:35	08:35:39	5	3902	32.6	9.1	7	7	100.0	100.0	100.0





21-07-07	17:31:38	18:31:29	60	3908	33.1	8.5	7	6	100.0	100.0	100.0
21-07-07	18:26:23	18:31:29	5	3908	33.0	8.6	6	5	100.0	100.0	100.0
22-07-07	08:55:08	09:55:07	60	3917	31.8	10.2	2	2	100.0	100.0	100.0
22-07-07	09:50:09	09:55:07	5	3917	32.5	9.3	4	4	100.0	100.0	100.0
22-07-07	17:10:58	18:10:45	60	3922	33.0	8.6	2	2	100.0	100.0	100.0
22-07-07	18:05:50	18:10:45	5	3922	33.8	7.7	2	2	100.0	100.0	100.0
23-07-07	08:34:29	09:34:27	60	3931	31.8	10.2	7	6	100.0	100.0	100.0
23-07-07	09:29:27	09:34:27	5	3931	32.5	9.3	7	7	100.0	100.0	100.0
23-07-07	16:50:02	17:50:03	60	3936	33.7	7.8	7	5	100.0	100.0	100.0
23-07-07	17:45:02	17:50:03	5	3936	33.3	8.3	7	5	100.0	100.0	100.0
24-07-07	08:13:44	09:13:44	60	3945	32.5	9.2	1	1	100.0	100.0	100.0
24-07-07	09:08:44	09:13:44	5	3945	33.3	8.3	6	6	100.0	100.0	100.0
24-07-07	16:29:22	17:29:23	60	3950	31.4	10.9	7	3	100.0	100.0	100.0
24-07-07	17:24:25	17:29:23	5	3950	33.2	8.4	7	5	100.0	100.0	100.0
25-07-07	07:53:01	08:52:59	60	3959	33.5	8.0	4	4	100.0	100.0	100.0
25-07-07	08:52:58	08:52:59	0	3959	33.0	8.7	6	6	100.0	100.0	100.0
25-07-07	17:48:49	18:48:49	60	3965	33.3	8.3	7	5	100.0	100.0	100.0
25-07-07	18:43:49	18:48:49	5	3965	32.4	9.4	7	6	100.0	100.0	100.0
26-07-07	07:32:12	08:32:12	60	3973	34.6	6.9	8	8	100.0	100.0	100.0
26-07-07	08:27:13	08:32:12	5	3973	32.9	8.7	7	7	100.0	100.0	100.0
26-07-07	17:28:01	18:28:02	60	3979	33.4	8.2	7	2	100.0	100.0	100.0
26-07-07	18:23:02	18:28:02	5	3979	33.0	8.6	7	1	100.0	100.0	100.0
27-07-07	07:12:22	08:11:21	59	3987	33.2	8.3	8	8	100.0	100.0	100.0
27-07-07	08:06:33	08:11:21	5	3987	34.0	7.4	7	7	100.0	100.0	100.0
27-07-07	17:07:20	18:07:19	60	3993	32.3	9.5	7	5	100.0	100.0	100.0
27-07-07	18:02:19	18:07:19	5	3993	32.9	8.7	6	1	100.0	100.0	100.0
28-07-07	08:31:22	09:31:00	60	4002	33.0	8.6	7	7	100.0	100.0	100.0
28-07-07	09:26:01	09:31:00	5	4002	32.9	8.7	6	6	100.0	100.0	100.0
28-07-07	16:46:37	17:46:37	60	4007	35.0	6.5	7	7	100.0	100.0	100.0
28-07-07	17:41:37	17:46:37	5	4007	32.9	8.7	6	6	100.0	100.0	100.0



29-07-07	08:10:18	09:10:17	60	4016	32.0	9.8	3	3	100.0	100.0	100.0
29-07-07	09:05:16	09:10:17	5	4016	33.9	7.5	3	3	100.0	100.0	99.7
29-07-07	18:06:12	19:06:10	60	4022	34.2	7.3	6	5	100.0	100.0	100.0
29-07-07	19:01:12	19:06:10	5	4022	34.9	6.6	7	6	100.0	100.0	100.0
30-07-07	07:49:32	08:49:32	60	4030	32.7	9.0	5	4	100.0	100.0	100.0
30-07-07	08:44:32	08:49:32	5	4030	34.5	7.0	7	5	100.0	100.0	100.0
30-07-07	17:46:52	18:45:22	59	4036	35.0	6.5	8	6	100.0	100.0	100.0
30-07-07	18:40:21	18:45:22	5	4036	36.0	5.6	7	4	100.0	100.0	100.0
31-07-07	07:28:45	08:28:44	60	4044	35.3	6.2	8	8	100.0	100.0	100.0
31-07-07	08:23:44	08:28:44	5	4044	37.4	4.7	8	8	100.0	100.0	100.0
31-07-07	17:25:21	18:24:36	59	4050	35.0	6.5	8	6	100.0	100.0	100.0
31-07-07	18:19:21	18:24:36	5	4050	34.8	6.7	6	7	100.0	100.0	100.0
01-08-07	08:48:15	09:48:15	60	4059	15.9	108.0	8	7	100.0	100.0	99.6
01-08-07	09:43:14	09:48:15	5	4059	36.7	5.1	8	7	100.0	100.0	100.0
01-08-07	17:03:46	18:03:52	60	4064	33.8	7.6	7	5	100.0	100.0	100.0
01-08-07	17:59:01	18:03:52	5	4064	24.4	30.2	7	3	100.0	100.0	100.0
02-08-07	08:27:35	09:27:34	60	4073	33.8	7.6	6	6	100.0	100.0	100.0
02-08-07	09:28:05	09:27:34	-1	4073	33.0	8.6	7	5	100.0	100.0	100.0
02-08-07	16:43:14	17:43:11	60	4078	32.8	8.8	8	4	100.0	100.0	100.0
02-08-07	17:38:11	17:43:11	5	4078	33.7	7.7	7	7	100.0	100.0	100.0
03-08-07	08:06:52	09:06:50	60	4087	33.3	8.3	7	7	100.0	100.0	100.0
03-08-07	09:01:50	09:06:50	5	4087	33.4	8.1	7	7	100.0	100.0	100.0
03-08-07	18:02:44	19:02:43	60	4093	33.8	7.7	7	1	100.0	100.0	100.0
03-08-07	18:57:43	19:02:43	5	4093	34.3	7.1	7	0	100.0	100.0	100.0
04-08-07	07:46:29	08:46:05	60	4101	34.2	7.1	8	4	100.0	100.0	100.0
04-08-07	08:41:26	08:46:05	5	4101	32.7	8.9	8	6	100.0	100.0	100.0
04-08-07	17:41:54	18:41:54	60	4107	33.3	8.1	7	7	100.0	100.0	100.0
04-08-07	18:36:54	18:41:54	5	4107	32.5	9.2	6	5	100.0	100.0	100.0
05-08-07	07:25:41	08:25:16	60	4115	33.7	7.6	8	2	100.0	100.0	100.0
05-08-07	08:21:11	08:25:16	4	4115	34.6	6.7	8	4	100.0	100.0	99.5



05-08-07	17:21:09	18:21:09	60	4121	34.1	7.2	7	1	100.0	100.0	100.0
05-08-07	18:16:09	18:21:09	5	4121	33.9	7.4	7	7	100.0	100.0	100.0
06-08-07	08:45:25	09:44:49	59	4130	32.8	8.7	2	2	100.0	100.0	100.0
06-08-07	09:40:12	09:44:49	5	4130	34.1	7.3	3	3	100.0	100.0	100.0
06-08-07	17:00:29	18:00:25	60	4135	29.9	13.2	7	1	100.0	100.0	100.0
06-08-07	17:58:41	18:00:25	2	4135	33.0	8.5	7	2	100.0	100.0	100.0
07-08-07	08:26:13	09:24:07	58	4144	32.2	9.5	2	0	100.0	100.0	100.0
07-08-07	09:20:50	09:24:07	3	4144	34.2	7.1	2	0	100.0	100.0	100.0
07-08-07	16:39:47	17:39:45	60	4149	33.0	8.4	2	0	100.0	100.0	100.0
07-08-07	17:34:37	17:39:45	5	4149	33.4	8.0	3	0	100.0	100.0	100.0
08-08-07	08:03:24	09:03:23	60	4158	33.2	8.3	1	0	100.0	100.0	100.0
08-08-07	08:58:23	09:03:23	5	4158	33.7	7.7	1	0	100.0	100.0	100.0
08-08-07	17:59:22	18:59:15	60	4164	32.7	8.8	1	1	100.0	100.0	100.0
08-08-07	18:55:16	18:59:15	4	4164	33.4	8.0	0	0	100.0	100.0	90.5
09-08-07	07:42:37	08:42:37	60	4172	33.9	7.5	7	1	100.0	100.0	100.0
09-08-07	08:37:37	08:42:37	5	4172	32.8	8.6	7	2	100.0	100.0	100.0
09-08-07	17:38:54	18:38:27	60	4178	34.1	7.2	5	3	100.0	100.0	100.0
09-08-07	18:33:20	18:38:27	5	4178	33.2	8.2	5	4	100.0	100.0	93.9
10-08-07	09:02:03	10:02:02	60	4187	31.4	10.5	3	3	100.0	100.0	100.0
10-08-07	09:57:02	10:02:02	5	4187	33.0	8.5	6	6	100.0	100.0	100.0
10-08-07	17:17:43	18:17:42	60	4192	32.3	9.4	7	7	100.0	100.0	100.0
11-08-07	08:41:22	09:41:22	60	4201	32.8	8.6	8	8	100.0	100.0	100.0
11-08-07	09:36:22	09:41:22	5	4201	32.3	9.3	8	8	100.0	100.0	99.9
11-08-07	16:56:59	17:56:59	60	4206	33.1	8.2	6	1	100.0	100.0	100.0
11-08-07	17:52:00	17:56:59	5	4206	32.8	8.6	6	1	100.0	100.0	99.2
12-08-07	08:20:41	09:20:41	60	4215	33.0	8.4	7	2	100.0	100.0	100.0
12-08-07	09:15:47	09:20:41	5	4215	34.0	7.3	7	2	100.0	100.0	100.0
12-08-07	16:36:18	17:36:18	60	4220	33.8	7.5	7	2	100.0	100.0	100.0
12-08-07	17:31:18	17:36:18	5	4220	33.1	8.3	4	1	100.0	100.0	100.0
13-08-07	07:59:58	08:59:56	60	4229	32.5	9.0	-999	7	100.0	100.0	100.0



13-08-07	08:54:53	08:59:56	5	4229	33.5	7.8	7	6	100.0	100.0	100.0
13-08-07	17:55:47	18:55:47	60	4235	34.6	6.7	7	7	100.0	100.0	100.0
13-08-07	18:50:46	18:55:47	5	4235	34.2	7.1	8	8	100.0	100.0	100.0
14-08-07	07:40:22	08:39:10	59	4243	34.5	6.8	8	8	100.0	100.0	100.0
14-08-07	08:35:12	08:39:10	4	4243	33.0	8.5	8	8	100.0	100.0	0.0
14-08-07	17:35:00	18:35:00	60	4249	33.0	8.3	4	2	100.0	100.0	100.0
14-08-07	18:30:01	18:35:00	5	4249	33.1	8.3	4	3	100.0	100.0	100.0
15-08-07	08:59:56	09:58:36	59	4258	33.3	8.0	8	8	100.0	100.0	100.0
15-08-07	09:53:29	09:58:36	5	4258	32.5	9.0	8	8	100.0	100.0	99.9
15-08-07	17:14:17	18:14:15	60	4263	32.4	9.0	7	7	100.0	100.0	100.0
15-08-07	18:09:15	18:14:15	5	4263	33.5	7.8	7	4	100.0	100.0	100.0
16-08-07	08:37:07	09:37:56	61	4272	34.6	6.6	7	1	100.0	100.0	100.0
16-08-07	09:32:09	09:37:56	6	4272	33.3	8.0	8	1	100.0	100.0	96.0
16-08-07	16:53:22	17:53:32	60	4277	33.9	7.3	8	4	100.0	100.0	100.0
16-08-07	17:57:12	17:53:32	-4	4277	34.0	7.2	8	4	100.0	100.0	96.2
17-08-07	08:17:12	09:17:14	60	4286	32.5	8.9	8	6	100.0	100.0	100.0
17-08-07	09:12:17	09:17:14	5	4286	33.9	7.4	7	6	100.0	100.0	96.2
17-08-07	16:32:35	17:32:52	60	4291	32.2	9.3	7	6	100.0	100.0	100.0
17-08-07	17:27:49	17:32:52	5	4291	33.9	7.4	7	7	100.0	100.0	95.1
18-08-07	07:56:10	08:56:29	60	4300	33.9	7.3	7	4	100.0	100.0	100.0
18-08-07	08:51:09	08:56:29	5	4300	35.7	5.7	7	5	100.0	100.0	93.0
18-08-07	17:52:19	18:52:19	60	4306	34.3	7.0	7	4	100.0	100.0	100.0
18-08-07	18:47:19	18:52:19	5	4306	33.7	7.6	7	2	100.0	100.0	100.0
19-08-07	07:35:09	08:35:42	61	4314	32.1	9.5	7	5	100.0	100.0	100.0
19-08-07	08:30:09	08:35:42	6	4314	12.4	180.9	6	3	100.0	100.0	100.0
19-08-07	18:26:32	18:31:32	5	4320	35.1	6.2	6	3	100.0	100.0	94.8
20-08-07	08:55:28	09:55:09	60	4329	32.1	9.4	7	7	100.0	100.0	100.0
20-08-07	09:50:11	09:55:09	5	4329	34.4	6.8	6	5	100.0	100.0	99.9
20-08-07	17:10:48	18:10:48	60	4334	32.8	8.5	3	3	100.0	100.0	100.0
20-08-07	18:05:48	18:10:48	5	4334	33.2	8.1	5	5	100.0	100.0	99.8



21-08-07	08:34:27	09:34:29	60	4343	34.2	6.9	1	1	100.0	100.0	100.0
21-08-07	09:29:31	09:34:29	5	4343	33.2	8.0	2	1	100.0	100.0	100.0
21-08-07	16:50:06	17:50:06	60	4348	32.6	8.7	3	1	100.0	100.0	100.0
21-08-07	17:45:06	17:50:06	5	4348	34.3	6.9	3	1	100.0	100.0	100.0
22-08-07	08:13:49	09:13:47	60	4357	35.1	6.0	7	5	100.0	100.0	100.0
22-08-07	09:08:47	09:13:47	5	4357	35.0	6.1	7	4	100.0	100.0	100.0
22-08-07	16:29:25	17:29:26	60	4362	34.6	6.5	5	3	100.0	100.0	100.0
22-08-07	17:24:35	17:29:26	5	4362	33.5	7.6	5	2	100.0	100.0	100.0
23-08-07	07:53:00	08:53:01	60	4371	34.1	6.9	7	4	100.0	100.0	100.0
23-08-07	08:48:01	08:53:01	5	4371	35.7	5.5	7	1	100.0	100.0	100.0
23-08-07	17:48:57	18:48:51	60	4377	34.5	6.6	7	4	100.0	100.0	100.0
23-08-07	18:43:48	18:48:51	5	4377	33.4	7.7	7	4	100.0	100.0	93.2
24-08-07	07:32:14	08:32:14	60	4385	33.3	7.9	1	0	100.0	100.0	100.0
24-08-07	08:27:15	08:32:14	5	4385	33.4	7.7	1	1	100.0	100.0	100.0
24-08-07	17:28:04	18:28:05	60	4391	33.7	7.4	7	3	100.0	100.0	100.0
24-08-07	18:23:04	18:28:05	5	4391	33.6	7.6	5	2	100.0	100.0	100.0
25-08-07	08:51:43	09:51:43	60	4400	34.2	6.8	8	8	100.0	100.0	100.0
25-08-07	09:46:44	09:51:43	5	4400	34.8	6.3	8	8	100.0	100.0	100.0
25-08-07	17:07:20	18:07:21	60	4405	2.4	737.5	8	3	100.0	100.0	100.0
25-08-07	18:02:20	18:07:21	5	4405	35.3	5.8	8	3	100.0	100.0	100.0
26-08-07	08:30:40	09:31:02	60	4414	32.8	8.3	7	7	100.0	100.0	100.0
26-08-07	09:26:34	09:31:02	4	4414	33.8	7.2	7	7	100.0	100.0	100.0
26-08-07	16:46:39	17:46:39	60	4419	33.4	7.6	7	7	100.0	100.0	100.0
26-08-07	17:41:40	17:46:39	5	4419	34.5	6.5	6	3	100.0	100.0	100.0
27-08-07	08:10:50	09:10:19	59	4428	33.3	7.6	6	4	100.0	100.0	100.0
27-08-07	09:05:13	09:10:19	5	4428	32.1	9.1	6	4	100.0	100.0	100.0
27-08-07	18:06:13	19:06:12	60	4434	34.8	6.2	6	3	100.0	100.0	100.0
27-08-07	19:01:12	19:06:12	5	4434	34.2	6.7	7	7	100.0	100.0	100.0
28-08-07	07:49:38	08:49:34	60	4442	33.3	7.5	5	5	100.0	100.0	100.0
28-08-07	08:44:46	08:49:34	5	4442	33.9	6.9	6	6	100.0	100.0	100.0



28-08-07	17:45:05	18:45:23	60	4448	32.3	8.7	6	4	100.0	100.0	100.0
28-08-07	18:40:37	18:45:23	5	4448	33.8	7.1	5	3	100.0	100.0	100.0
29-08-07	07:28:54	08:28:46	60	4456	33.5	7.3	7	2	100.0	100.0	100.0
29-08-07	17:24:55	18:24:37	60	4462	32.9	8.1	7	3	100.0	100.0	100.0
29-08-07	18:20:02	18:24:37	5	4462	34.8	6.1	7	2	100.0	100.0	100.0
30-08-07	08:49:05	09:48:16	59	4471	32.7	8.3	7	7	100.0	100.0	100.0
30-08-07	09:43:19	09:48:16	5	4471	35.1	5.9	7	7	100.0	100.0	100.0
30-08-07	17:03:54	18:03:54	60	4476	32.1	9.0	3	2	100.0	100.0	100.0
30-08-07	17:58:53	18:03:54	5	4476	32.9	8.0	4	1	100.0	100.0	100.0
31-08-07	08:27:35	09:27:35	60	4485	33.2	7.6	6	6	100.0	100.0	99.9
31-08-07	09:22:36	09:27:35	5	4485	34.0	6.9	5	4	100.0	100.0	100.0
31-08-07	16:43:12	17:43:12	60	4490	33.1	7.8	4	2	100.0	100.0	100.0
31-08-07	17:38:22	17:43:12	5	4490	33.3	7.6	4	2	100.0	100.0	100.0
01-09-07	08:06:53	09:06:52	60	4499	31.8	9.4	6	2	100.0	100.0	100.0
01-09-07	09:01:51	09:06:52	5	4499	32.3	8.8	5	2	100.0	100.0	100.0
01-09-07	18:02:46	19:02:44	60	4505	33.5	7.3	3	3	100.0	100.0	100.0
01-09-07	18:57:46	19:02:44	5	4505	33.1	7.8	2	2	100.0	100.0	100.0
02-09-07	07:46:05	08:46:06	60	4513	33.4	7.5	5	0	100.0	100.0	100.0
02-09-07	08:41:05	08:46:06	5	4513	32.1	9.0	7	1	100.0	100.0	100.0
02-09-07	17:41:57	18:41:56	60	4519	34.0	6.9	6	2	100.0	100.0	100.0
02-09-07	18:36:55	18:41:56	5	4519	33.7	7.2	5	1	100.0	100.0	100.0
03-09-07	07:26:05	08:25:17	59	4527	33.4	7.4	7	5	100.0	100.0	100.0
03-09-07	08:20:17	08:25:17	5	4527	36.0	5.2	7	6	100.0	100.0	100.0
03-09-07	17:21:09	18:21:10	60	4533	33.9	7.0	7	7	100.0	100.0	100.0
03-09-07	18:16:11	18:21:10	5	4533	34.3	6.5	8	8	100.0	100.0	100.0
04-09-07	08:44:26	09:44:50	60	4542	32.6	8.4	5	4	100.0	100.0	100.0
04-09-07	09:39:42	09:44:50	5	4542	33.7	7.1	6	5	100.0	100.0	100.0
04-09-07	17:00:26	18:00:26	60	4547	33.6	7.2	6	1	100.0	100.0	100.0
04-09-07	17:55:26	18:00:26	5	4547	34.0	6.8	7	1	100.0	100.0	100.0
05-09-07	08:24:10	09:24:08	60	4556	33.2	7.7	4	0	100.0	100.0	100.0



05-09-07	09:19:10	09:24:08	5	4556	33.7	7.1	6	1	100.0	100.0	100.0
05-09-07	16:39:42	17:39:46	60	4561	35.1	5.8	8	8	100.0	100.0	100.0
05-09-07	17:34:41	17:39:46	5	4561	31.1	10.4	7	7	100.0	100.0	99.5
<b>Type of sounding:</b>							<b>Cloudiness:</b>				
	PTU							0 - 2			
	Ozone							3 - 6			
	CFH							7 - 8			